International Journal of Earth Sciences
https://doi.org/10.1007/s00531-020-01911-y

ORIGINAL PAPER

An andesitic sill complex in the Southern Permian Basin: volcanogenetic model and stratigraphic implications

Ludwig Luthardt[1] · Christoph Breitkreuz[1] · Joerg W. Schneider[1,2] · Birgit Gaitzsch[1,2] · Judith Brink[3] · Klaus Peter Stanek[1] · Ulf Linnemann[4] · Mandy Hofmann[4] · Bodo-Carlo Ehling[5]

Received: 16 March 2020 / Accepted: 11 July 2020

Abstract

Subvolcanic intrusions are highly variable in shape and structure, and occur in nearly all parts of the upper crust, as a result of extensive volcanic activity. Processes of subvolcanics interacting with the host rock are insufficiently understood, as they are rarely exposed. In the southernmost part of the Flechtingen-Altmark Subprovince, (sub)volcanic rocks of the Flechtingen Volcanic Complex (FVC) are exposed in several quarries. It is built up of silicic tuffs, ignimbrites and lava flows, but also of intermediate lavas and extended sill sheets. Additionally, major granitic intrusions exposed by drillings are associated with the FVC. In the Mammendorf quarry, a sill intruded in between lithified turbiditic series of early Carboniferous (Visean–Serphukovian) age at the base, and widely consolidated volcanoclastic deposits of late Carboniferous (late Pennsylvanian) age at the top. Various magma-host rock interactions were found indicating brittle and ductile deformation patterns occurring at the basal contact, and secondary fluidal mixing predominantly occurring at the top contact, most probably caused by fluids accompanying the intruding magma. We present an extended volcanogenetic model for the FVC. Volcanic activity initiated at 302 ± 3 Ma with fallout deposits represented by mostly re-deposited silicic ashfall deposits of the Flechtingen Formation, and cumulated in depositing major ignimbrite series, most likely forming a caldera. Later, the sills intruded at the rheological boundary of the lithified Mississippian turbiditic series and the partly consolidated volcanoclastic series. Finally, major granitic intrusions emplaced in the basement rocks at around 298 ± 4 Ma. The study contributes to clarify stratigraphic constraints of late Carboniferous to early Permian continental deposits and sheds light on stratigraphy of significant late Paleozoic volcanic deposits of the Flechtingen-Altmark Subprovince in the Southern Permian Basin.

Keywords Southern Permian Basin · Late Paleozoic volcanism · Andesite · Sill · Peperite · Caldera

Introduction

The Variscan continent–continent collision and following extensional tectonics in Europe (e.g. Kroner et al. 2016) was related to intensive late- to post-orogenic magmatism (Timmerman 2008; von Seckendorff 2012; Repstock et al. 2018; Fig. 1a). Large caldera-forming systems (Marx et al. 1995, Benek et al. 1996; Hoffmann et al. 2013; Repstock et al. 2018; Casas García et al. 2019) and siliceous lava complexes (Korich 1992; Paulick and Breitkreuz 2005; Geißler et al. 2008) are important elements. Subvolcanic activity played also a prominent role in some of the late Paleozoic intramontane basins (Obst and Katzung 2000; Awdankiewicz et al. 2004; Breitkreuz and Mock 2004; Lorenz and Haneke 2004; Schmiedel et al. 2015; Breitkreuz et al. 2018).

Post-collisional volcanic activity in the Saxothuringian domain initiated in the late Mississippian by the formation

✉ Ludwig Luthardt
l.luthardt@gmx.de

[1] Geological Institute, Technische Universität Bergakademie Freiberg, Bernhard-von-Cotta, Straße 2, 09599 Freiberg, Germany

[2] Kazan Federal University, 18 Kremlevskaya Str., Kazan 420008, Russian Federation

[3] Oststraße 2, 09599 Freiberg, Germany

[4] Senckenberg Naturhistorische Sammlungen Dresden, GeoPlasma Lab, Königsbrücker Landstraße, 159, 01109 Dresden, Germany

[5] Landesamt für Geologie und Bergwesen (LAGB), Sachsen-Anhalt, Köthener Straße 38, 06118 Halle, Germany

Published online: 28 July 2020

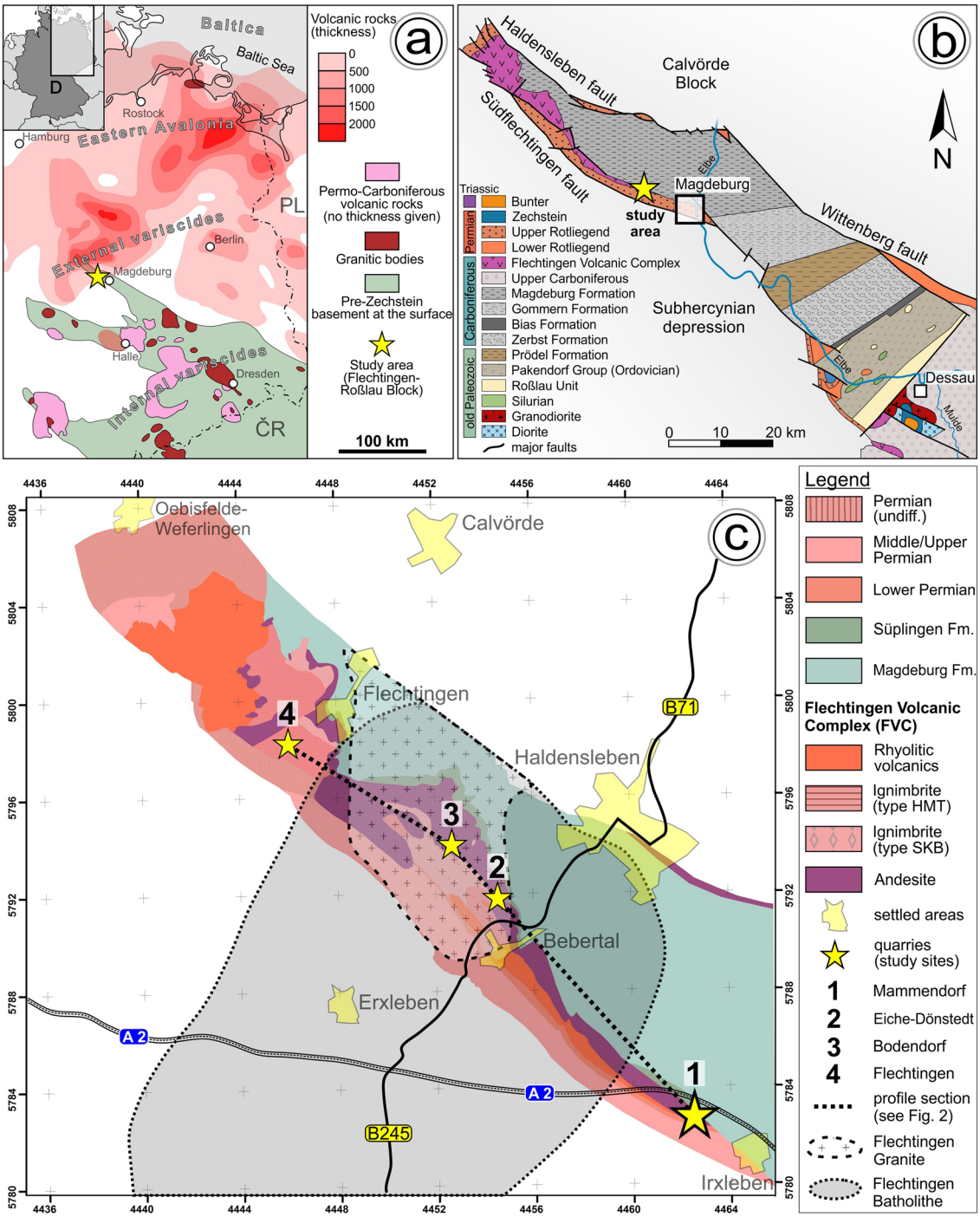

Fig. 1 Geography and geology of the study area: **a**) distribution and thickness variations of late Paleozoic magmatic rocks in Central Europe (modified from Benek et al. 1996); **b** Geology of the Flechtingen–Roßlau Block showing middle to late Paleozoic sedimentary and volcanic units with oldest units in the south-eastern part and younger units towards north-western direction due to tectonic uplift (after https://www.regionalgeologie-ost.de); **c** Geological details of the Flechtingen Volcanic Complex in the north-western part of the Flechtingen–Roßlau Block and outcrop areas from this study and Awdankiewicz et al. (2004): *HMT* Holzmühlenthal, *SKB* Steinkuhlenberg; extension of the Flechtingen and Roxförde Granites after Söllig and Röllig (1989)

of the Altenberg–Teplice Volcanic Complex (Hoffmann et al. 2013; Casas García et al. 2019). Its climax took place at the Carboniferous–Permian transition near the Variscan orogenic front and in the foreland to the North (Benek et al. 1996; Breitkreuz et al. 2007), presumably controlled by dextral transpression/transtension (Arthaud and Matte 1977),

as well as extension and rifting (Förster and Romer 2010; Kroner and Romer 2013). Intensive volcanism continued throughout the early Permian, in particular in the intra-montane basins (Lorenz and Haneke 2004; Hoffmann et al. 2013; Repstock et al. 2018, 2019). Small-volume basaltic eruptions occurred during the middle to late Permian Havel and Elbe Subgroups in the Southern Permian Basin (Gebhardt et al. 1991; Benek et al. 1996; Geißler et al. 2008).

In the geological framework of the Variscan to post-Variscan tectonic development in Central Europe, the Flechtingen–Roßlau Block (FRB) in central Germany represents the temporal and regional linkage between the molasse facies of the intra-montane basins of the Variscan orogen in the South, and the widely distributed post-Variscan late Carboniferous to Permian successions in the North German Basin (Gaitzsch et al. 1995). The FRB is the only outcrop area of voluminous volcanic successions of the North-East German Large Igneous Province (NEGLIP, Paulick and Breitkreuz 2005) that have been discovered in 3000–8000 m depth during hydrocarbon exploration drilling in the second half of the twentieth century in north-eastern Germany and western Poland (Hoth et al. 1973; Benek et al. 1996; Geißler et al. 2008). Benek et al. (1996) estimated a volume of c. 48,000 km^3 for the German part. NEGLIP is dominated by ignimbrite sheets, silica-rich lava dome/laccolith complexes and Mg-andesite shield volcanoes (Geißler et al. 2008). U/Pb dating of zircon revealed volcanic activity between 303 and 290 Ma, with a proposed maximum between 299 and 295 Ma (Breitkreuz et al. 2007). Based on outcrops and drillings, Benek et al. (1996) estimated a volume of 13,840 km^3 of preserved volcanics in the Flechtingen-Altmark Subprovince, which includes the FRB.

The late Carboniferous to early Permian Flechtingen Volcanic Complex (FVC) is the northernmost outcrop of late Paleozoic volcanism in Central Europe (Fig. 1a, 3) and represents a large caldera complex (Gersemann 1989, Benek et al. 1995) with associated major granitic intrusions of Flechtingen, Roxförde and Velpke-Asse D1 (Kelch and Paulus 1980). It started with minor SiO_2-rich explosive eruptions, followed by the deposition of voluminous rhyolitic welded to non-welded ignimbrites (Benek et al. 1973, 1996). The FVC forms part of the Altmark Subgroup where numerous hydrocarbon exploration wells (e.g. Salzwedel 2/64) detected extensive and thick sheets of welded ignimbrites and granites of late Carboniferous to early Permian age (Stedingk et al. 1997; Breitkreuz and Kennedy 1999; Breitkreuz et al. 2007). According to Geißler et al. (2008), volcanism in the Flechtingen-Altmark Sub-Province was dominated by ignimbrite-forming eruptions contributing to a levelling of the palaeo-landscape.

The Flechtingen ignimbrites comprise the non-welded, lithic-rich Steinkuhlenberg unit and the welded Holzmühlental unit (Benek et al. 1973, 1996). The latter stands out for the occurrence of garnet (Geißler et al. 2008), assumed to represent a co-magmatic phase in the anatectic zone of the lower crust. Garnet-bearing volcanics, known also from other late Paleozoic volcanics in Europe (Gilbert and Rogers 1989; Geißler et al. 2008), are typical for calc-alkaline, early post-collisional magmatism (Harangi et al. 2001). The deposition of the up to 650 m thick Flechtingen ignimbrites was followed by the intrusion of voluminous andesitic magma into unconsolidated volcanoclastic sediments below the pyroclastic sheet (Awdankiewicz et al. 2004). The nearly synchronous emplacement of voluminous rhyolitic pyroclastics and andesitic subvolcanics may point to a simultaneous presence of large, essentially independent magma reservoirs in the lower crust (Kennedy et al. 2018).

Based on outcrops in the active quarries of Eiche–Dönstedt and Bodendorf, and on exploration wells, Awdankiewicz et al. (2004) were the first to prove a subvolcanic nature of the voluminous andesites below the Flechtingen ignimbrites. This conclusion was supported by detailed observations at the top contact of the andesite body (Eiche–Dönstedt quarry, and drillings) and by the presence of meter-sized sedimentary rafts in the andesite (mainly in the Bodendorf quarry). The top contact of the Eiche–Dönstedt quarry comprises small magmatic apophyses into the host sediments, fluidisation of host sediments, missing top breccia, and a graben-and-horst geometry of some segments of the contact (Fig. 2). The sedimentary rafts represent bridges between longitudinally and laterally propagating protolobes of the sill (Hutton 2009).

In this contribution, a detailed facies analysis is presented from a coherent andesite body and the under- and overlying sediments exposed in the Mammendorf quarry, located c. 12 km to the Southeast of the Eiche–Dönstedt quarry (Figs. 1c, 3). Based on fieldwork, studies on rock slabs, drill cores, and thin sections, we attempt to substantiate the subvolcanic facies for the andesite body and discuss its geometry and intrusive mechanisms. In synthesis with new radiometric ages of associated pyroclastics and hidden granitic bodies, we provide new implications on magma genesis, stratigraphy and regional geology of the FVC.

Geological setting

The FRB depicts a Northwest–Southeast trending block with an extension of 30 × 95 km (Fig. 1b). The block was obliquely lifted up as a result of the compressional tectonic regime during the alpine orogeny in the late Cretaceous to early Cenozoic (Brink 2005; Bachmann et al. 2008). Sedimentary and (sub-) volcanic rocks of Neoproterozoic to late Paleozoic age are cropping out at the surface of the FRB. Frequently, these rocks are unconformably overlain by marine sediments of the Cenozoic (e.g., Müller 2011)

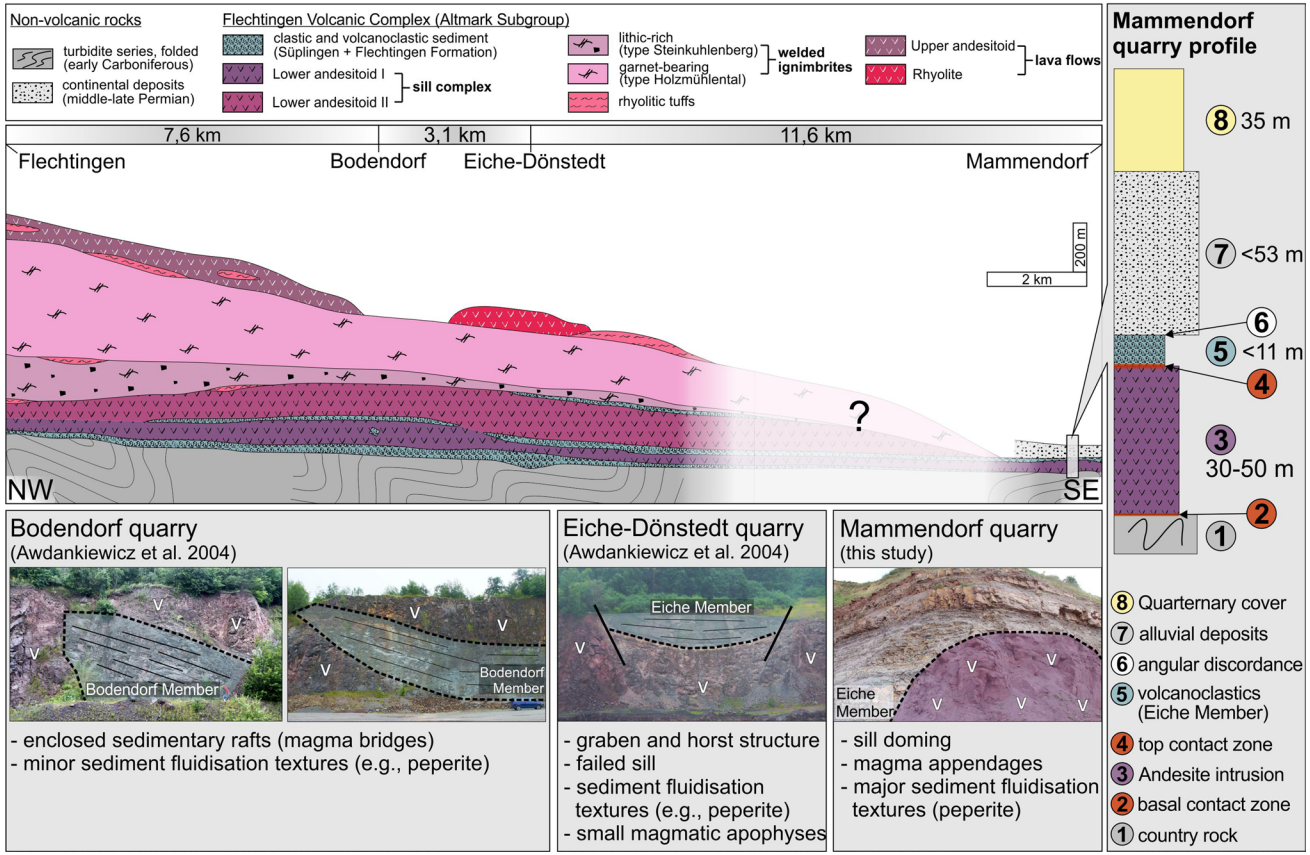

Fig. 2 Schematic facies architecture of volcanic and volcano-sedimentary units of the FVC in a vertical section (modified and extended from Benek et al. 1973). See Fig. 1 for profile line; images from the quarries show large-scale sediment-magma interaction caused by the sill intrusion

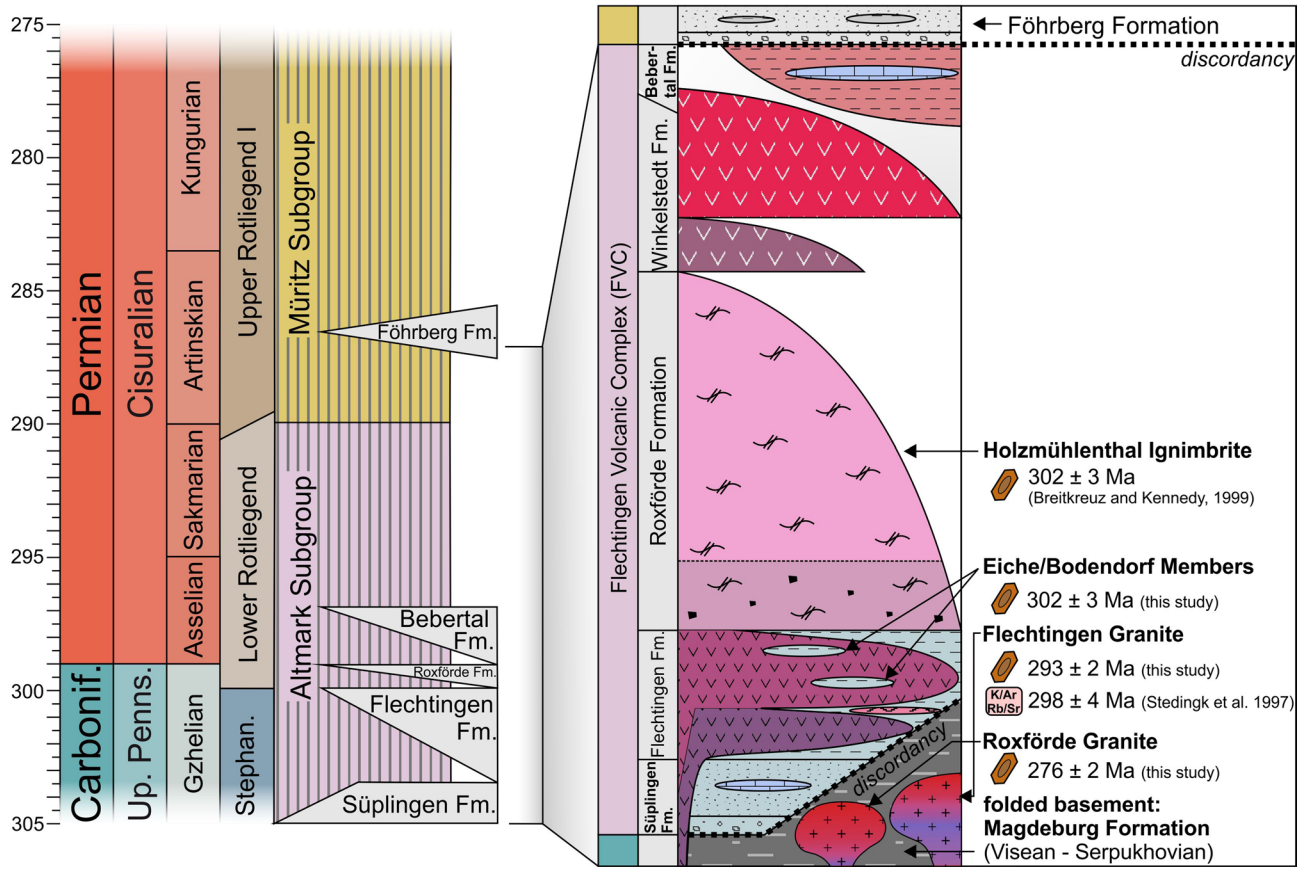

Fig. 3 Stratigraphy of the Altmark Subgroup and Flechtingen Volcanic Complex (FVC). Left: stratigraphy after German Stratigraphic Chart (2016) and Schneider et al. (2019); Right: stratigraphy modified from Gaitzsch et al. (1995). See Fig. 2 for lithology and classification

and glacial sediments of the Quaternary (Litt and Wansa 2008). Besides numerous exploration drillings, the middle to late Paleozoic succession is partially exposed in several quarries (Eiche–Dönstedt, Bodendorf, Flechtingen) in the north-western part of the FRB. The Mammendorf quarry, west of Magdeburg, opened in 1998 and is among the most important outcrops, as it exposes the south-easternmost part of this succession with three major stratigraphic units: (1) early Carboniferous marine deposits, (2) late Carboniferous to early Permian (sub-) volcanics of the FVC, and (3) middle to late Permian clastic continental deposits. Drillings in the FRB revealed the presence of the Flechtingen Granite (Well Flechtingen 1/82) and the Roxförde Granitoid (Roxförde 2/62), which both have emplaced into early Carboniferous meta-sediments (Bauer et al. 1995).

Palaeozoic country rock: early Carboniferous marine deposits

The marine successions of early Carboniferous (Mississippian) age represent the country rock in the Mammendorf quarry and are part of the eastern Rhenohercynian fold and thrust belt (Bachmann et al. 2008; Fig. 1b). The sedimentary units represent molasse deposits of the eroding Variscan orogen and are stratigraphically subdivided into the Pakendorf Group, as well as Prödel, Zerbst, Bias, Gommern and Magdeburg Formation (Bachmann et al. 2008). The whole succession is dominated by small-scaled rhythmic deposits of normally graded clastic sediment of poor maturity. Single layers are in average few decimetres thick and composed of sandstone/fine conglomerates at the base and clay-/siltstone layers at the top. As the strata exhibit scour marks caused by streaming water, sub-autochthonous faunal elements (e.g., trilobites, goniatites, conodonts) and allochthonous floral elements in the silt layers, the deposits have been clearly interpreted as marine turbiditic sequences of the Gondwana/Laurussia foreland basin (Paech 1973). Based on marine faunal elements, the succession has been dated to Visean–Serpukhovian age (Paech 1973; Weyer 1975). Under Variscan compression, the strata became deformed into wide W–E and ENE–WSW trending folds.

Flechtingen Volcanic Complex (FVC) and associated sediments

The (sub-)volcanic rocks of late Paleozoic age are found at the surface in the southwestern part of the FRB (Fig. 1b, c). These units of latest Carboniferous to early Permian age are part of the Altmark Subgroup (Fig. 3), which represents a c. 1500 m thick succession of pyroclastic and volcanic rocks of basic to rhyolitic composition (Marx et al. 1995; Benek et al. 1996; see Fig. 2). These have been subdivided into a pre-, syn- and post-ignimbritic phase (Benek et al. 1973). The volcanic rocks are interpreted to be deposited during a voluminous eruption, associated with the formation of a large caldera (Marx et al. 1995). The eruption centre is suggested to be in the Northwest of the town of Flechtingen, as in this area the succession has its maximum thickness (Benek et al. 1973). The eruption phases are assigned to four formations (Flechtingen, Roxförde, Winkelstedt, Bebertal Fm.), each representing deposits of volcanic and (volcano-) clastic material resulting from different eruption intervals (Gaitzsch et al. 1995). However, recent results distinctly show that re-interpretation of the stratigraphic units is mandatory (e.g., Awdankiewicz et al. 2004, this study). Thus, the stratigraphic order displayed below needs prospective revision.

At the base of the Altmark Subgroup, the Süplingen Formation is seen as a separate stratigraphic unit (German Stratigraphic Chart 2016; Fig. 3). The Süplingen Fm. discordantly overlies the folded marine sedimentary country rock of early Carboniferous (Visean–Serphukovian) age. The up to 70 m thick series consists of sandstones, greywackes and siltstones with intercalated dm-thick micritic lacustrine limestones and rarely rhyolitic crystal tuff horizon (Paech et al. 1973; Gaitzsch et al. 1995). Isolated wedge-shaped occurrences of basal conglomerates could indicate relief gradients of the palaeo-surface, as their components are dominated by local country rock. Sedimentary structures such as drag marks, flute moulds and striation patterns point to temporally streaming water bodies, whereas raindrop-like patterns were interpreted as gas deflation structures in a flat, standing water body (Paech et al. 1973). The fossil record comprises floral elements (*Walchia piniformis*, *Cordaites* sp., *Samaropsis*, *Neuropteris planchardii*, *Odontopteris osmundaeformis*, *Annularia stellata*, *Sphenopteris* sp.; Kahlert 1973), and in the thin lacustrine limestones ostracods and gastropods (Gebhardt 1988). Frequently occurring domains of thermal overprint are described for the Süplingen Formation and characterised by contact metamorphic minerals, such as lime-silicates and epidote, potentially resulting from a granitic intrusion (Hoth et al. 1973; Paech et al. 1973). Based on the megafloral composition, a Gzhelian (Stephanian C) to Asselian age was assumed (Kahlert 1973).

The following Flechtingen Fm. was first assumed to represent the initial magmatic phase of the Flechtingen volcanic activity as it is composed of two major andesitic units ("older andesitoid I" and "II"), which were interpreted as initial lava flows (Paech et al. 1973). The "lower (older) andesitoid I" is 30–100 m thick and characterised by an aphyric, crystal-poor fabric and a lack of quartz. The "lower andesitoid II" has a maximum thickness of 150 m and contains up to 20 vol.% of quartz crystals (Benek et al. 1973). These intermediate rocks are geochemically classified as tholeiitic trachy-andesites (Benek et al. 1996). In between or trapped within the andesitoids, the isolated volcanosedimentary Bodendorf and Eiche members occur, which remain stratigraphically poorly defined (Gaitzsch et al. 1995). These members bear several fossil remains including plant foliage impressions, arthropod traces (*Diplichnites minimus*, Walther and Gaitzsch 1988) and limnic bivalves. Later, Awdankiewicz et al. (2004) studied the basal and top contacts of the andesitic bodies in the Bodendorf, Eiche and Dönstedt quarries (Fig. 1c) and resumed that these "lava flows" most likely represent subvolcanic intrusions, which have been emplaced as sills in the series of poorly lithified volcanoclastic sediments (Süplingen Fm. + Eiche/Bodendorf members). The authors described planar, sharp contacts of the sill and host rocks, but also various structures of magma-host rock interactions, such as fault-bounded grabens at the top, failed sills, perlites and peperites (Fig. 2). In the result, the volcanogenic model of the FVC was modified, as these sills are believed to have been intruded during the post-ignimbritic phase.

The syn-ignimbritic phase after Benek et al. (1973) is represented by two ignimbrite varieties of the Roxförde Formation with a wide distribution in the FRB and a maximum thickness of 650 m (Fig. 2). In contrast to the upper variety (Holzmühlental ignimbrite), the basal variety (Steinkuhlenberg ignimbrite) has an increased percentage of lithic fragments (15–25%) and a potassium feldspar/plagioclase ratio > 1 (Benek et al. 1973). During the eruption, the geochemical composition changed from rhyolitic (Steinkuhlenberg ignimbrite) to increasingly andesitic (Holzmühlental ignimbrite). The latter variety bears up to 20 grains of magmatic garnet per 100 cm^2 (almandin, Geißler et al. 2008). Both ignimbrites are interpreted as hot pyroclastic flow deposits, as distinct fiamme and spherulites indicate welding compaction. The Holzmühlental ignimbrite has been radiometrically dated to an age of 302 ± 3 Ma (Gzehlian), based on U/Pb dating on zircon (Breitkreuz and Kennedy 1999).

Rhyolitic lava flows and ignimbrites, as well as sheets of andesite ("upper andesitoids") are part of the overlying Winkelstedt Formation. The "upper andesitoids" are interpreted as plugs and lava domes or short flows (Benek et al. 1973; Awdankiewicz et al. 2004) and represent extrusiva of the post-ignimbritic phase.

The volcanic succession is completed by a c. 75 m thick series of clay-/siltstones with intercalated rhyolitic to dacitic tuff horizons. They represent the product of the youngest eruptions of the FVC during the post-ignimbritic phase. The sediments are part of the Bebertal Formation (Gaitzsch et al. 1995), bearing several mesophilic floral elements, such as *Autunia naumannii*, *Walchia piniformis* and *Odontopteris lingulata* (Barthel et al. 1982) and faunal elements, such as xenacanthid and amblypterid fish remains (Gaitzsch et al. 1995).

Middle to late Permian continental deposits

Siliciclastic sediments of middle to early late Permian age (Upper Rotliegend II) are overlying the volcanoclastic and sub-volcanic units of the Altmark Subgroup by an erosional discordancy. These deposits are clearly of non-volcanic origin and indicate a hiatus in the sedimentary record of more than 20 million years during the early to middle Permian. The Upper Rotliegend II deposits at Mammendorf consist of conglomerates, sandstones and clay-/siltstones, which build up at least three fining-up cycles (each < 10 m thick) in the lower part of the profile. In certain levels of these cycles, assemblages of tetrapod footprints and invertebrate burrows were found (Buchwitz et al. 2017). Towards the top, silt- and sandstones are dominant, showing pedogenic overprint, which is indicated by colour mottling and carbonate nodules/cementation. These clastics represent fluvial deposits of a wadi system in the southern border area of the mega-playa system of the Southern Permian basin (Legler 2006; Legler et al. 2011).

Material and methods

New results on the andesitic sill system and its host rocks presented in this study are predominantly derived from the Mammendorf quarry in northern central Germany (N 52° 10′29.84″/E 11° 26′ 15.92″). Currently, the quarry has an extension of 817 vs. 372 m and a maximum depth of ca. 70 m. Data were collected during geological mapping and a bachelor study in 2012–2013 (Brink 2013; Luthardt 2013). The investigations are based on vertical and lateral outcrop documentation from six levels in the quarry, but also on drill core documentation of seven exploration wells in the vicinity of the quarry. Rock samples were taken from all lithological units to produce polished rock slabs and thin sections. With regard to their mineral content and fabrics, thin sections were qualitatively and quantitatively analysed using a cross-polarised microscope. Geometric reconstruction of the sill system was performed by combining outcrop data from several quarries and drillings in a NW–SE oriented profile (Figs. 1c + 2).

To unravel the radiometric age of the late Pennsylvanian volcanoclastic host rocks, rock material from a crystal-rich rhyolitic tuff in the Mammendorf quarry was collected. Zircon concentrates were separated from c. 2 kg sample material using standard methods. Samples for the radiometric ages of the granite intrusions originate from drill cores. For the Flechtingen Granite, the sample Flech-1 was analysed from the well Flechtingen 1/82 (N 52°19′ 22.18″/E 11° 14′ 15.30″/106.8 m NN), taken at a depth of 473 m. For the Roxförde Granite, the sample Rox-1 was analysed from the well Roxförde 2/62 (N 52° 28′ 13.06″/E 11° 26′ 4.48″/65 m NN) at a depth of 2848 m. For all three samples, final selection of the zircon grains for U–Pb dating was achieved by hand-picking under a binocular microscope. Around 120 zircon grains of all grain sizes and morphological types were selected, mounted in resin blocks, and polished to half their thickness. The laser points with concordant ages used for the age calculation were marked in the homogeneous core of long prismatic to needle-shaped crystals, which appear as middle grey domains in the CL images (Fig. 6; Suppl-Fig. 1).

Zircons were analysed for U, Th, and Pb isotopes by LA-SF ICP-MS techniques at the Museum für Mineralogie und Geologie (GeoPlasma Lab, Senckenberg Naturhistorische Sammlungen Dresden) using a Thermo-Scientific Element 2 XR sector field ICP-MS (single-collector) coupled to a RESOlution 193 nm excimer laser. Each analysis consisted of approximately 15 s background acquisition followed by 30 s data acquisition, using a laser spot-size of 25 and 35 µm, respectively. A common-Pb correction based on the interference- and background-corrected ^{204}Pb signal and a model Pb composition (Stacey and Kramers 1975) were carried out if necessary. The necessity of the correction is judged on whether the corrected ^{207}Pb/^{206}Pb lies outside of the internal errors of the measured ratios (Frei and Gerdes 2009). Discordant analyses were generally interpreted with care. Raw data were corrected for background signal, common Pb, laser-induced elemental fractionation, instrumental mass discrimination, and time-dependant elemental fractionation of Pb/Th and Pb/U using an Excel® spreadsheet program developed by Axel Gerdes and Richard Albert Roper (Institute of Geosciences, Johann Wolfgang Goethe-University Frankfurt, Frankfurt am Main, Germany). Reported uncertainties were propagated by quadratic addition of the external reproducibility obtained from the standard zircon GJ-1 (~0.6% and 0.5–1% for the ^{207}Pb/^{206}Pb and ^{206}Pb/^{238}U, respectively; Jackson et al. 2004) during individual analytical sessions and within-run precision of each analysis. To

test the accuracy of the measurements and data reduction, we included the Plesovice zircon as a secondary standard in our analyses. Here, reproducibly ages of c. 337 Ma were measured, fitting with the results of Sláma et al. (2008). Concordia diagrams (2σ error ellipses) and concordia ages (95% confidence level) were produced using Isoplot/Ex 2.49 (Ludwig 2001), and frequency and relative probability plots using AgeDisplay (Sircombe 2004). The $^{207}Pb/^{206}Pb$ age was taken for interpretation for all zircons > 1.0 Ga, and the $^{206}Pb/^{238}U$ ages for younger grains. For further details on analytical protocol and data processing see Gerdes and Zeh (2006). Zircons showing a degree of concordance in the range of 90–110%, are classified as concordant (e.g., Meinhold et al. 2011), because of the overlap of the error ellipse with the concordia. U and Pb content and Th/U ratio were calculated relative to the GJ-1 zircon standard and are accurate to approximately 10%. Analytical results of U–Th–Pb isotopes and calculated U–Pb ages are given in supple_tables 1–3 (see supplement).

Results

The stratigraphic succession in the Mammendorf quarry is composed of five major lithological units (Fig. 2). At the base of the quarry, marine turbiditic clastic sediments of early Carboniferous age are exposed showing tectonic folding. The early Carboniferous units were originally overlain by a series of volcanoclastic sediments of assumed late Pennsylvanian age. In between these two units, the basic to intermediate andesite body is located. At the base and the top of the andesite, different structures at the magma-sediment contact occur.

The volcanogenic sediments are discordantly overlain by alluvial sediments of Upper Rotliegend II stratigraphic age. Finally, unconsolidated relics of coastal marine sediments of the Oligocene (Müller 2011) and glacial/inter-glacial sediments of Quaternary age discordantly overlie the whole succession in the outcrop.

Early Carboniferous sedimentary succession

In the outcrops of the Mammendorf quarry, dark grey to reddish greywacke is exposed, showing a rhythmic interbedding of sand-/fine gravel strata and clay-rich siltstone, whereas single layers are up to few decimetres thick. Biogenic components, such as calamite axes, are rare.

Based on composition and sedimentary structures, the succession is interpreted as a turbidite sequence of the Magdeburg Formation (Visean–Serphukovian). Variscan compressional tectonic processes led to folding and faulting of the sediments, which is clearly demonstrated in the outcrop. Close to the andesite contact, up to 10 cm large cooling columns were formed, indicating heating and cooling of the sedimentary rock.

Late Carboniferous volcanoclastics

At the top of the andesite body, a series of volcanogenic fine-grained clastics was documented (Fig. 4). The succession has a variable thickness of up to eleven metres in the outcrop, showing a slight erosional and angular top contact to the middle-upper Permian coarse-grained deposits. The volcanogenic succession is dominated by sandy clay-/siltstones, which appear in the outcrop as greyish-violet to greenish and predominantly horizontally bedded sedimentary rocks (Fig. 4a, b). Occasionally, low-angle trough bedding is present. The partially volcanogenic origin is evidenced by blocky to vesicular shards (Fig. 4e), as well as by mm-sized collapsed pumice fragments. Clastic components are of low maturity encompassing subangular quartz, lithics and dispersed mica (Fig. 4h). Originally, the fabric of the sedimentary succession was dominated by a fine horizontal stratification with normal gradation within the laminae (Figs. 4d, 5c). Frequently, the original stratification is reworked forming rip-up-like clasts (Fig. 4d). Tepee-like structures are interpreted as syn-sedimentary water-escape structures (Fig. 4d). Rarely, decimetre-thick, very well sorted and massive sandstone lenses are intercalated in the middle part of the succession (Fig. 4g, c). The sand grains show a quartzitic fabric within a silicate matrix (Fig. 4f). These lenses represent minor channel fill deposits, which were overprinted by high-temperature diagenesis. Several horizons contain fossil remains, such as plant impressions (e.g., roots, fern leaves, calamite axes), but also trace fossils, e.g. undulating drag marks of unknown swimming producers.

Towards the top of the succession in the southwestern part of the quarry, a 0.2 m thick, locally restricted crystal-rich tuff was documented (Fig. 6). It represents a moderately sorted pyroclastic rock with a greenish matrix and white altered feldspar crystals (Fig. 6a, b). The matrix is composed of altered vesicular shards and small pumice fragments. Components are (hyp-)idiomorphic alkali feldspars, hypidiomorphic quartz crystals, lithic fragments, plagioclase and accessory minerals such as zircon and sulfides. The (hyp-)idiomorphic feldspar crystals show strong alteration overprint, due to diagenetic overprint (Fig. 6b). Zircon grains selected and measured from this horizon reveal a U/Pb radiometric age of 302 ± 3 Ma (Fig. 6c, d). The spectrum of zircons from the fine-grained rock sample comprises short to long prismatic crystals between 80 and 200 µm size. Only a few needle-shaped zircons occur. Many zircons yield a U-rich core surrounded by a U-poor rim yielding magmatic zonation. Due to the fact that many zircons had a disturbed isotopic system, further analysis on inherited zircon remains speculative. There seem to be some with an age of

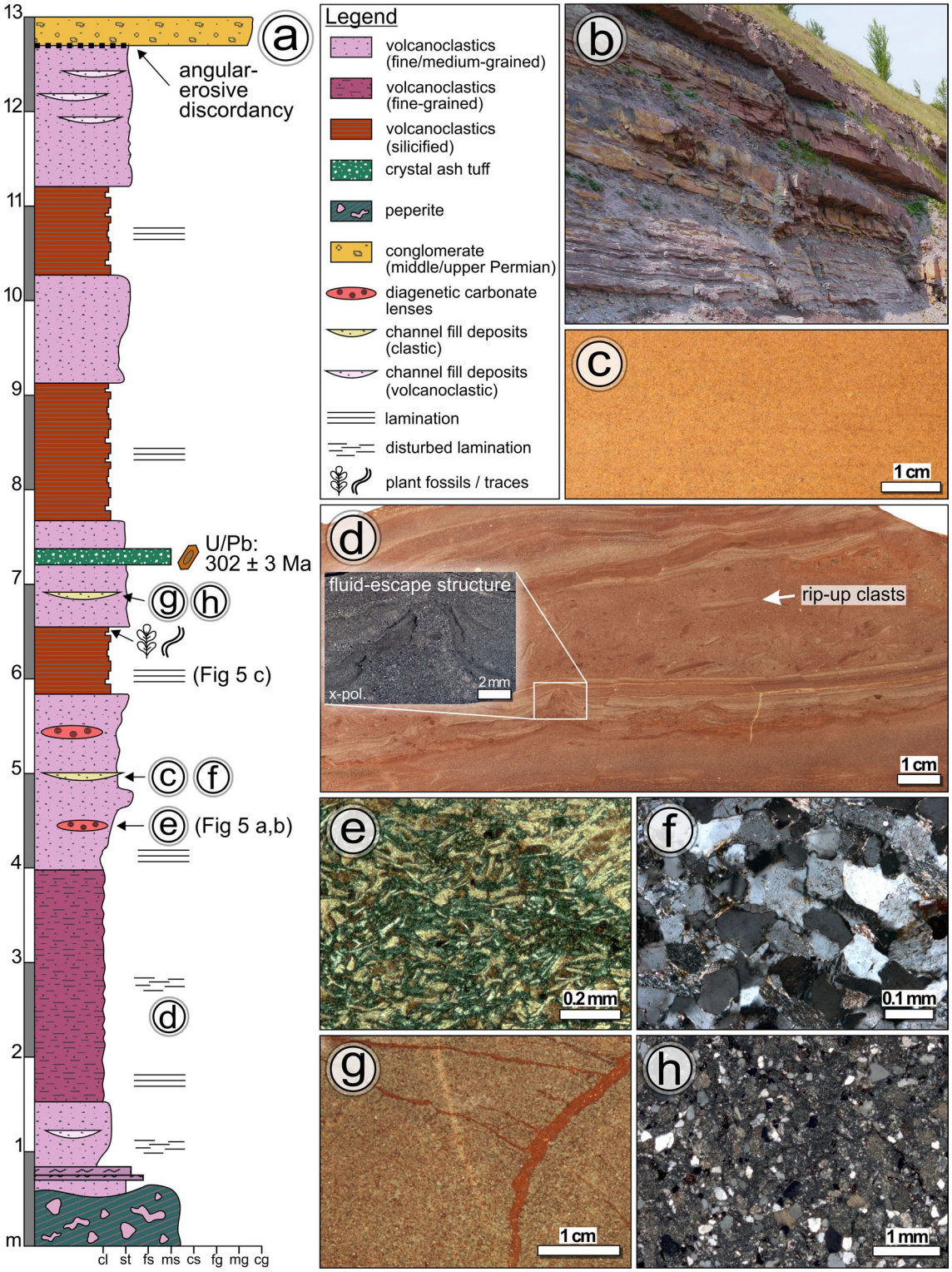

Fig. 4 Characterisation of the volcano-sedimentary host rock (Eiche Member, Flechtingen Formation) at the top of the sill in the Mammendorf quarry. **a** Normalised profile section in the quarry exposing the maximum thickness of 11 m. **b** Horizontally bedded sediment in the outcrop; **c** mature clastic channel-fill deposit from the mid part of the profile; **d** typical fabric of the volcano-sediment from the basal part of the profile showing disturbed horizontal lamination with rip-up clasts and syn-sedimentary fluid escape structure (zoom from thin section under cross-polarised light); **e** dominating volcanic glass shards in a diagenetic carbonate lens demonstrating the partially high amount of volcanic components; **f** mature quartz grains with quartzitic fabric in a thin section from "**c**"; **g** coarse-grained, well-sorted and silicified channel-fill deposits from the mid part of the section with haematitic veins; **h** immature composition of the sediment shown in "**g**"

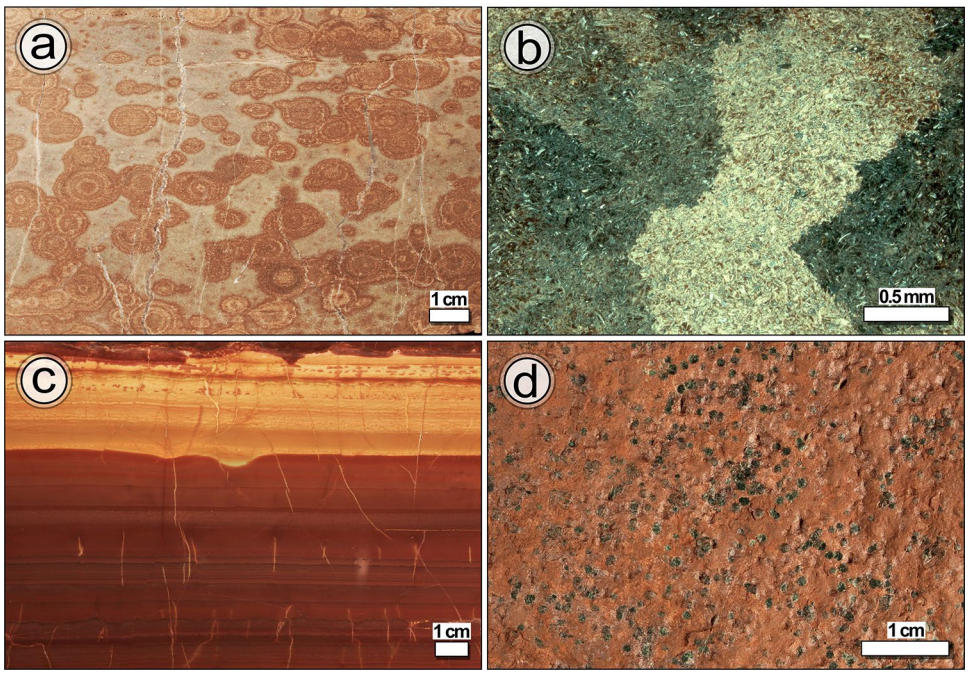

Fig. 5 Indications of hydrothermal overprint in the volcano-sedimentary succession. **a** Concentric haematite growth zones in a carbonate cemented lens (see Fig. 4); **b** coarse sparitic carbonate cement (dolomitic) in the same carbonate lens from "**a**"; **c** silicified fine-grained sediment from jasper-like horizons (Fig. 4), showing original lamination; **d** cleavage plane of laminated sediment at the top of a silicified horizon with numerous chlorite grains

325–330 Ma, whereas zircon of Cadomian age is exceptionally rare.

The volcanoclastic succession is interpreted as a series of predominantly reworked pyroclastics with a moderate non-volcanic clastic input, but also in-situ pyroclastic fallout horizons. The predominantly ash-sized pyroclastic material is most probably derived from medial to distal fallout deposits. The in-situ pyroclastic horizons represent ash fall deposits produced by explosive rhyolitic volcanism. Some of them are likely to have been deposited underwater in a temporary lake or pond (e.g. Fig. 5c). The volcanoclastics were predominantly deposited in a fluvio-lacustrine facies association. Syn-sedimentary water escape structures, trace fossils and minor channel deposits point to temporal, shallow standing water bodies, with phases of subaerial exposition.

The volcanoclastic series shows further characteristics of secondary thermal overprint and fluid migration. The original fine horizontal stratification of the succession is frequently fragmented showing in part fluid-escape structures, which indicate an upward migration of post-sedimentary fluids (Fig. 4d). In the lower part of the profile, lens-shaped carbonate domains with up to 5 cm wide zones of concentric haematite rings are documented (Fig. 5a). The carbonate appears as coarse sparitic cementation of the matrix, in which volcanic glass shards were preserved (Fig. 5b). Towards the top of the volcanogenic series, several metre-thick, strongly silicified jasper-like horizons occur (Fig. 5c). These are banded, intensely reddish-brown coloured and composed exclusively of microcrystalline quartz/chalcedony. The banded colouring is referred to the preservation of lamination in the original sediment. At the top of these horizons, dark green sphere-shaped chlorite frequently occurs on the layer surfaces (Fig. 5d).

Andesitic magmatic body

The magmatic rock material represents a grey to violet coloured, crystal-poor andesite exhibiting a microcrystalline groundmass. Matrix is composed of fine needle-shaped feldspar crystals. Idiomorphic and prismatic phenocrysts, predominantly plagioclase, occur as accessory components. Thus, the volcanic rock is the most likely product of a basic to intermediate melt, which rapidly cooled down after emplacement. The absence of quartz phenocrysts and the small size of groundmass crystals are specific characteristics described for the "older andesitoid I" in the north-western FRB (Benek et al. 1973).

In the Mammendorf quarry, the magmatic body may be described as a more or less sheet-like rock body with an average thickness of 40–50 m in the study area, decreasing eastwards down to 25 m. Further east of the study site, it completely disappears, most probably due to (palaeo-) erosion, which is evidenced by exploration drillings. The andesite boundaries are more or less wavy-shaped at the basal contact and slightly irregular at the top contact with occasional bulge-like doming, several metres high (Fig. 2). In the outcrop, the andesite occurs as a homogeneous magma body. Gaseous vesicles are dominant at the top of the body but are distinctly decreasing in frequency towards the base. Contrary, the vesicle size decreases from the base (max. 15 cm) towards the top (1–2 cm). Secondarily, the vesicles were filled by fluids resulting in the crystallization of calcite,

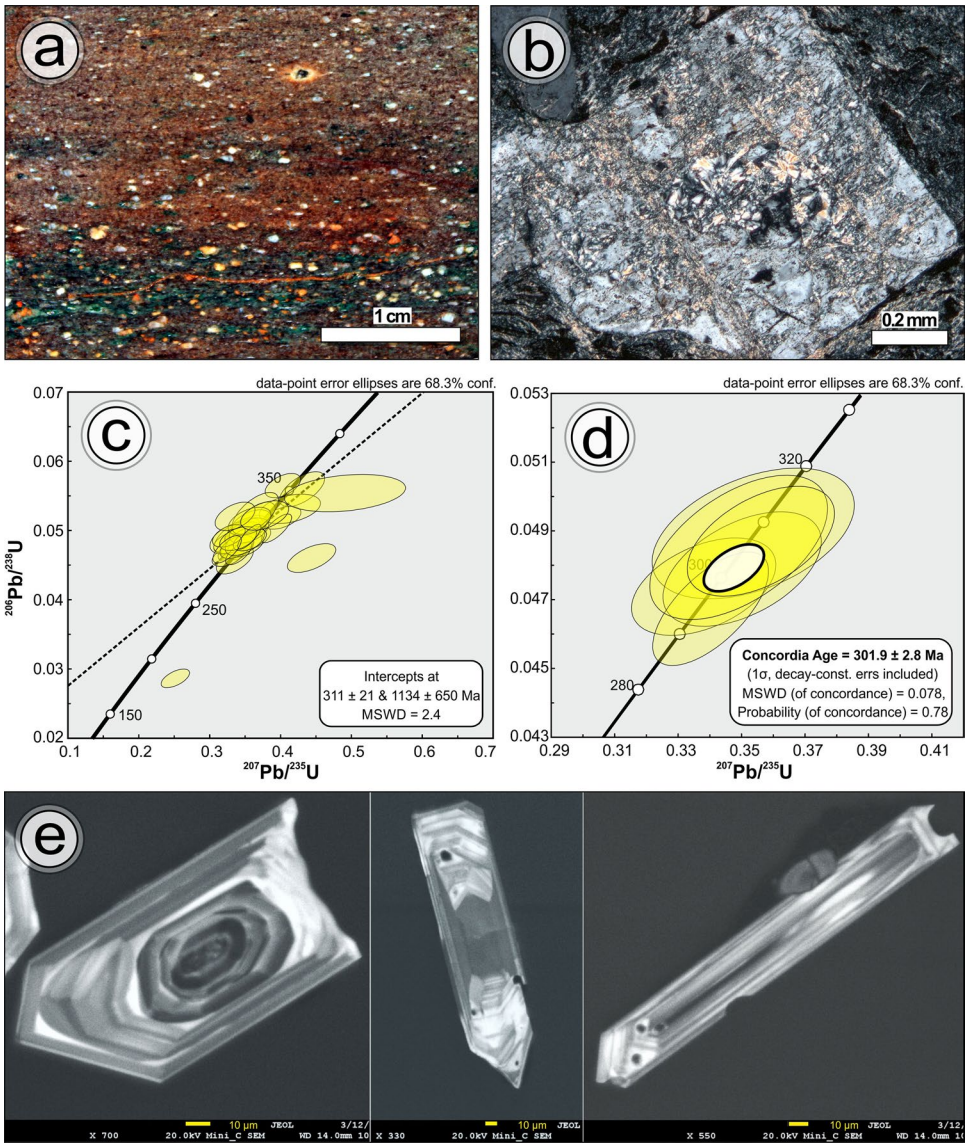

Fig. 6 Radiometric dating on the crystal tuff of the volcanoclastic series in the Mammendorf quarry. **a** rock section shows a green matrix and light-coloured altered feldspar crystals; **b** highly altered feldspar crystal (cross-pol.); **c** Concordia plot of all zircons from the Mammendorf sample, showing slightly disturbed isotopic systems at the majority of zircons; **d** Concordia plot of eight selected zircons with magmatic zonation; **e** back-scattered SEM images from examples of the shape and zonation of zircon selected for the age interpretation in Fig. 6d

haematite and chalcedony. Elongation of the vesicles results from shear stress produced by the flowing magma at the top. Distinct vertical cooling joints were documented at the basal contact with the early Carboniferous turbidites.

Andesite–host rock contacts

Due to different physical properties of the above described sedimentary units, the basal and top contact of the magma body show different magma-sediment textures. The basal contact of the andesite with turbiditic sedimentary rocks of early Carboniferous age is dominated by an irregularly-shaped morphology resulting in thickness variations of the andesite of up to several metres. The contact zone is of various thickness (< 0.9 m) and might be missing at some places (Fig. 7a), where the contact is very sharp and shows no major interactions of magma and host rock (Fig. 7e). Where the contact zone is present, it reveals a fragmented appearance (Fig. 7b). It consists of andesitic juvenile clasts, smaller fragments of the country rock and a greenish-reddish sediment, which is rich in secondary haematite (Fig. 7d). The andesitic juvenile clasts are few centimetres large, angular-shaped, vesicle-rich and frequently fragmented in situ. Millimetre-thick calcite veins are abundant in the whole contact zone. In some places, the original fabric of the country rock is fragmented, whereas a greenish to reddish-haematitic sediment occurs in the fissures and fractures (Fig. 7c). In between these fissures and fractures, light-red coloured andesitic magma veins are present, in some areas replacing the sediment.

The top contact zone of the magma body and the late Pennsylvanian volcanoclastic strata exhibits, with one exception, a regular shape. The exception depicts a tens of metres large bulge that pierced several horizons of the overlying

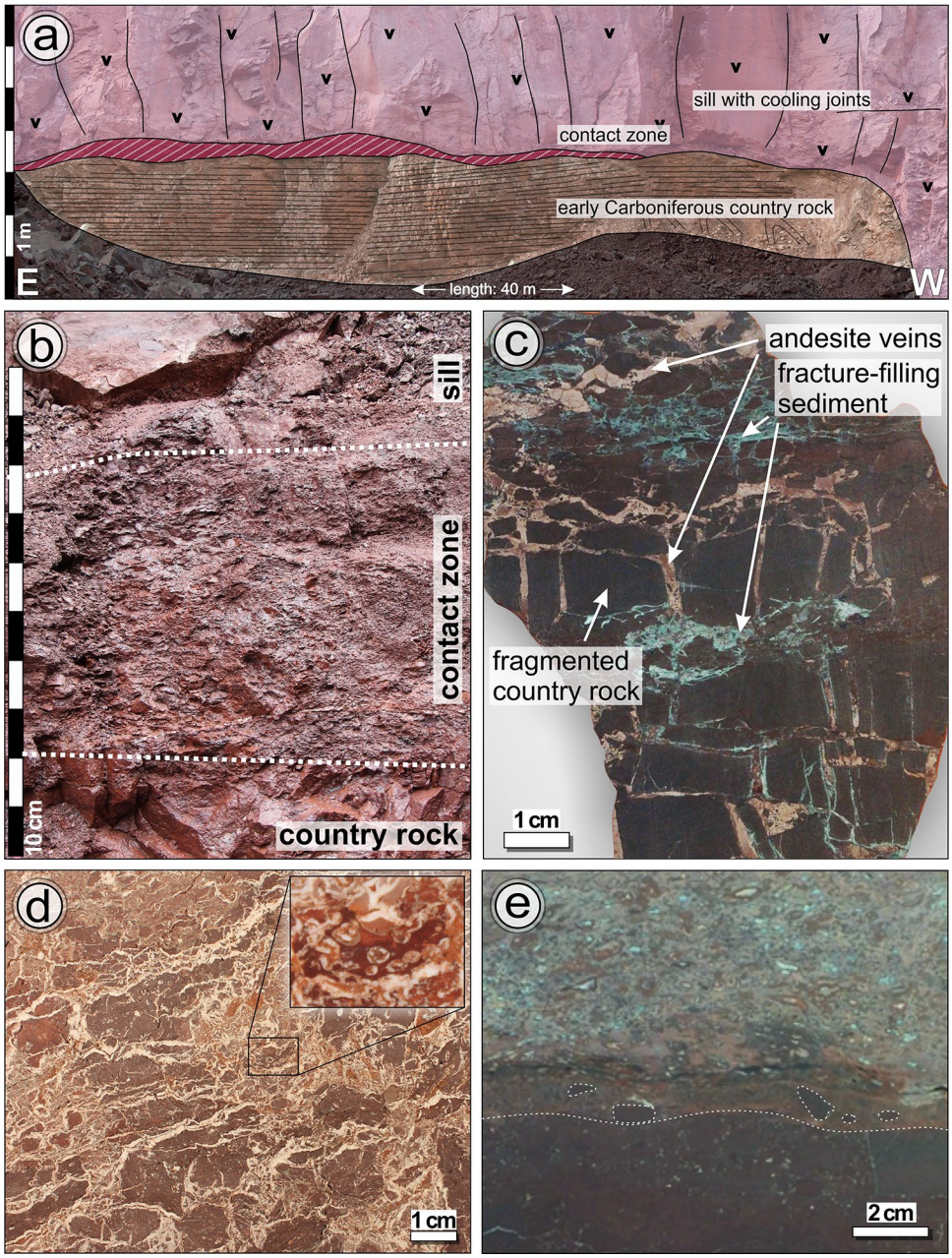

Fig. 7 Sill contact with the basal host rock (early Carboniferous turbidites) in the Mammendorf quarry: **a** outcrop situation at the quarry base exposing the contact zone (dark grey area not exposed); **b** detail of the contact zone in the same outcrop; **c** rock section of the basal contact zone showing andesite that had been squeezed in between fissures of the decomposed host rock (sample MD 4); **d** rock section showing sediment-magma interactions (peperite) in the contact zone with angular, vesicle-rich, andesitic juvenile clasts (dark violet, see close-up), sedimentary matrix (light colours) and abundant calcite veins; **e** rock section of the direct basal contact where a contact zone is missing: andesite (greenish-grey) at the top and early Carboniferous host rock (dark reddish colour) at the base showing a sharp transition with some small host-rock clasts.

volcanoclastic units (Figs. 2, 8a). At the top, an up to five metres long apophyse-like magmatic appendage occurs (Fig. 8a). At the same time, the volcanoclastic succession was slightly lifted up by the magma. In general, the contact of the andesite and the volcanoclastics depicts a sediment-magma mixing zone with a thickness of 0.5–3.2 m (Fig. 8b, c). It reveals typical properties of a peperite (Skilling et al. 2002), as it is composed of a sedimentary matrix and andesitic juvenile clasts. The matrix is composed of the dark greenish-grey, strongly consolidated clay-/siltstone of volcanoclastic origin. Haematite frequently occurs either inter-granular or in crystallisation domains (Fig. 8e). In the matrix, the original stratification of the sediments becomes more indistinct and finally disappears towards the direct andesite contact, which is interpreted as a result of fluidisation of unconsolidated sediment (Fig. 8b). Fluidal mixing processes are further indicated by detrital mica plates, which are mostly oriented parallel to the surface of the andesite juvenile clasts. The latter are up to 0.3 m in diameter and have fluidal, subangular, blocky and elongated morphologies with fractured, irregular margins (Fig. 8b–d). Glassy margins are missing in the clasts. Clast concentration and size are high at the magma boundary and decrease with increasing distance from the contact (Fig. 8b, c). The juvenile clasts exhibit a high vesicle density, whereas the vesicles are partly filled with volcanoclastic matrix material. At microscopic scale, matrix material of the sediment intruded along fine fissures into the vesicles (Fig. 8f). Both in macroscopic and

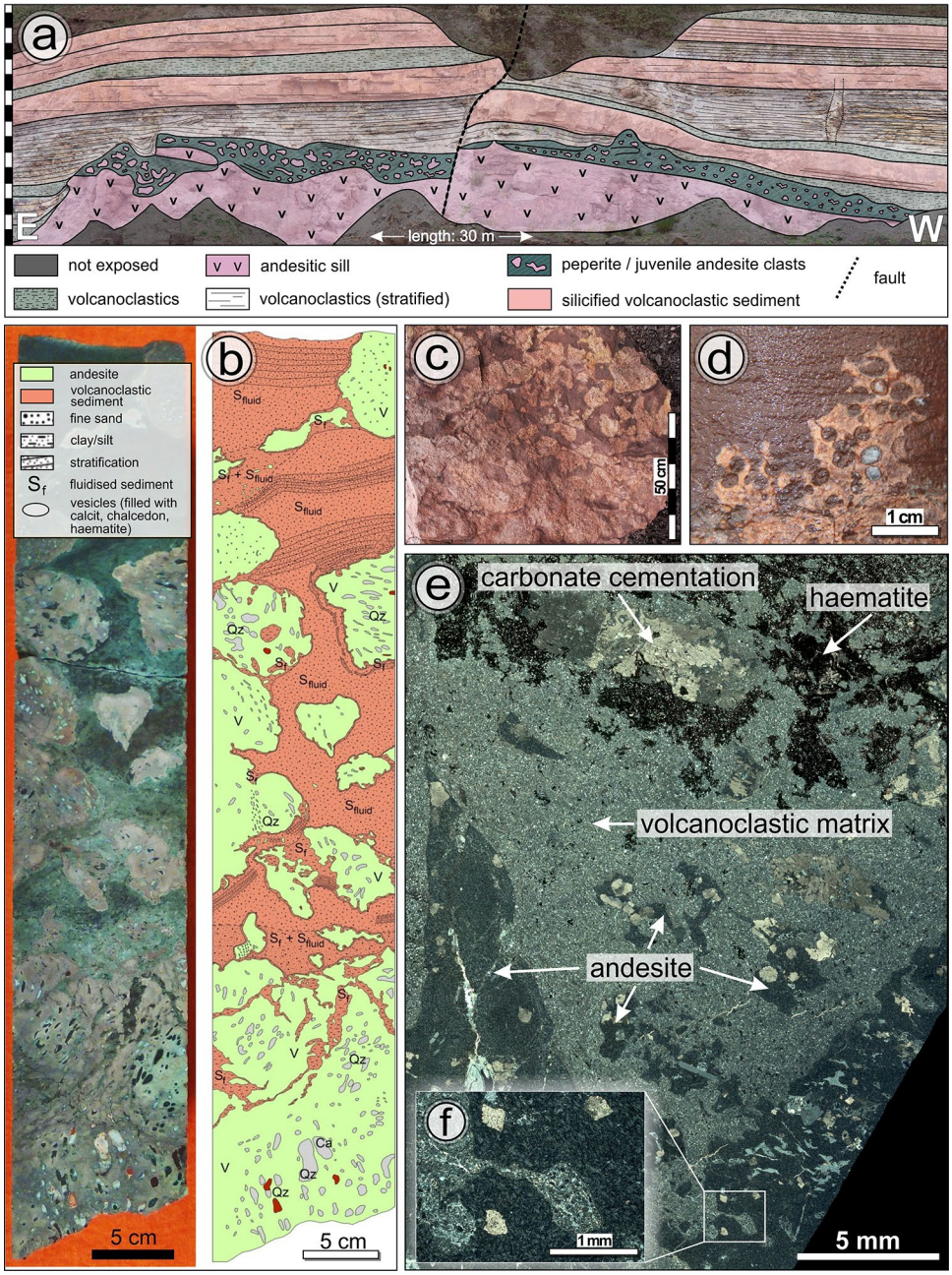

Fig. 8 Top contact of the sill with volcanoclastic sediment in the Mammendorf quarry. **a** Outcrop situation at the top showing the sill doming upwards in the host rock; **b** section of a drill core (Mam 13/12) with peperitic structures at the contact zone (notice sediment fluidisation structures and residual layering of the host rock); **c** contact zone in a block showing that andesitic juvenile clasts decrease in size and frequency with increasing distance from the sill; **d** pumice-like clast with sediment-filled vesicles indicating hydromagmatic explosions in the sediment; **e** thin section under cross-polarised light from the peperite for details of sediment-magma interaction and hydrothermal fluidal overprint; **f** sediment-filled vesicle illustrating fragmentation of juvenile clasts by hydromagmatic explosions

microscopic scale, an in-situ fragmentation of the juvenile clasts, most probably as a result of gas explosions or quenching, has been documented (Fig. 8e).

Discussion

New data from the Mammendorf quarry reveal that the andesite body of this outcrop represents a concordant sill, which intruded in between the early Carboniferous marine turbidites and the volcanoclastic series. The results give further support for the sill intrusion model proposed by Awdankiewicz et al. (2004) for the FVC. Consequently, the sill intrusion model for the whole sill system is extended. Further, new aspects of the volcanogenic model of the FVC are supposed. Finally, inferences on the (volcano-)stratigraphy of the FVC and FRB are discussed.

Sill intrusion modelling

In addition to drillings and outcrops in the Bodendorf/Dönstedt/Eiche quarries described by Awdankiewicz et al. (2004), the Mammendorf quarry represents the south-easternmost outcrop of FVC sub-volcanic rocks (Fig. 1), and

thus provides new insights into their geometry, structure and distribution at their distalmost part related to the volcanic centre (see below). Due to the distal position, the sill is relatively thin (25–50 m) in the Mammendorf quarry, compared to the north-western FRB (thickness of up to 200 m, Awdankiewicz et al. 2004; Fig. 2). In general, the sill complex was intruding below and into the series of volcanoclastic sediment (Eiche Member), thus showing a strata-concordant morphology. Nevertheless, local varieties occur in the adjacent outcrops. The andesite sill in the Mammendorf quarry is interpreted to represent the equivalent of the quartz phenocryst-free "older andesitoid I" described by Benek et al. (1973). Thus, in contrast to the other quarries, only the lower variety of the sill complex occurs in the Mammendorf quarry, exhibiting the widest extension of both varieties in south-eastern direction with > 25 km (Fig. 2). Presumably, the more differentiated quartz-phyric "lower andesitoid II" had a higher viscosity impeding a comparably extensive lateral propagation.

In contrast to other outcrops, the Mammendorf quarry currently exposes both, the lower and upper contact of the sill ("lower andesitoid I"): the early Carboniferous marine sedimentary rocks and the basal volcanoclastics of the FVC, respectively. Both sedimentary units show major differences in their rheologic behaviour during the intrusion. Hence, the sill complex intruded both along a stratigraphic and rheologic rock boundary. The basal contact appears quite complex, which is due to the fact that three major rock components were involved: andesitic magma, early Carboniferous country rock and a non-lithified, in part fracture-filling sediment (Fig. 7c). The latter may either represent an in-situ substrate produced by physical and chemical surface weathering during exposure of the country rock, or the basal layers of the overlying volcanoclastic series, or a mix of both. Where the magma interacted with the non-lithified sediment, a contact zone, here interpreted as a blocky peperite (compare to Busby-Spera and White 1987; Gihm and Kwon 2017), was formed. In the peperite auto-brecciation of blocky juvenile clasts (Fig. 7d) indicates mechanical stress caused by magmatic/fluid gas explosions (Skilling et al. 2002). In rare places, magmatic veins injected sediment-filled fissures of the fractured country rock due to vertical emplacement stress of the sill (Fig. 7c). As the fractures and fissures were already filled by sediment, it is highly suggestive that the early Carboniferous country rock was already fractured long before the intrusion, probably as a result of physical weathering during exposure. Where the sediment is absent, the sharp contact between andesite and host rock (Fig. 7e) indicates a solid, lithified state of the early Carboniferous turbiditic series at the time of intrusion.

Magma–host rock interactions at the top contact differ in part from the basal one and are throughout characterised by a well-developed peperite (White et al. 2000; Brown and Bell 2007). Juvenile clasts with fluidal to sub-planar morphologies indicate intense magma-sediment mingling (Fig. 8). The compact shape and the fractured margins of the clasts suggest that the andesitic magma was highly viscous. Most probably, clast fragmentation took place in the ductile–brittle transitional regime, predominantly caused by hydromagmatic explosions, but also by quenching (jigsaw fit clasts) and/or mechanical shear stress (elongated clasts; Skilling et al. 2002). Magma-sediment mingling resulted from fluidisation, as corresponding textures are ubiquitous, e.g. sediment textural homogenisation, sediment-filled vesicles and hairline cracks (Skilling et al. 2002), as well as obliquely uplifted sedimentary slabs (Kokelaar 1982). It is suggestive that the volcanoclastic host sediment was partially consolidated when the sill intruded. In the Bodendorf quarry, a large sedimentary slab (> 8 × 3 m) has been trapped in between two proto-lobes (Awdankiewicz et al. 2004; Fig. 2). It is interpreted as a "broken bridge", which finally developed from overlapping, propagating and inflating magma segments as a result of brittle deformation during emplacement of a sill (Hutton 2009). Moreover, Awdankiewicz et al. (2004) interpreted a graben/horst structure at the top contact of the sill in the Eiche quarry as an interaction with the rigid host rock. In the Mammendorf quarry, partial uplift of the volcanoclastic succession accompanied by faulting (Fig. 8a) infers slightly brittle deformation of the host rock, in response to rapidly increasing vertical stress created by doming of the intrusion (Schofield et al. 2012; Haug et al. 2017). Altogether, we assume that the volcanoclastic series had been consolidated at the time of intrusion, but not lithified, because soft-sedimentation (peperite) widely occurs. The latter is most abundant in the Mammendorf quarry, suggesting that the degree of consolidation was lower compared to the volcanoclastics in the other outcrops. These local differences may be referred to different intrusion depth related to the coverage by the voluminous ignimbrites of the Roxförde Formation, which are not known in the Mammendorf area (Fig. 1c, 3). Presumably, the ignimbrite thickness was distinctly lower in the distal area of the Mammendorf quarry, leading to a dominance of soft-sediment deformation.

Based on a comparison of the host–sediment rheological behaviour in the Eiche–Dönstedt and Bodendorf quarries (brittle deformation, magma fingers, broken bridge) with other sill systems worldwide (Schofield et al. 2012), a maximum intrusion depth of around 2 km is assumed. Awdankiewicz et al. (2004) suggested an intrusion depth of 600–800 m for the Bodendorf and Eiche–Dönstedt quarries. Based on the maximum thickness of the overlying ignimbrites of the Roxförde Formation, a maximum intrusion depth of 600 m may be realistic.

Hydrothermal activity accompanied by sill intrusions is well-known from several localities (Jamtveit et al. 2004;

Svensen et al. 2018). Here, the effects of fluid mobilisation during intrusion and cooling are obvious in the volcanoclastic host sediments. Vertical fluid escape structures in the sedimentary layers suggest upward migration of fluids (Fig. 4d). Sill-related fluid migration facilitated the growth of secondary minerals in the volcanoclastic series, encompassing (1) matrix-forming haematite concentrated close to the sill contact (Fig. 8e), (2) carbonate lenses in the lower part of the succession with concentric haematite rings (Figs. 4a, 5a), (3) sandstone channel fill deposit with quartzitic fabric (Fig. 4f) and (4) small knots of manganese oxides and chlorite (Fig. 5d). Jasper-like silicified horizons found in the volcanoclastics of the Mammendorf quarry (Fig. 5c) are also referred to fluidal impact. Similar silicified tuff horizons in the FRB were also described by Schreiber (1960) who interpreted them as being formed by hot silicic fluids as a result of volcanic activity. Hoth et al. (1973) found further secondary minerals such as epidote, garnet, pyrite along tiny veins and calc-silicate nodules in the Süplingen Formation and the early Carboniferous country rock, which they interpreted as contact metamorphic products of deep-seated intermediate magmatic intrusions. However, growth of these minerals could also be referred to the sill-related thermo-fluidal overprint.

Stratigraphic implications

The stratigraphy of the FRB and the FVC is still based on the old volcanogenetic model, in which the andesite magmatic sheets have been interpreted as lava flows (e.g., Benek et al. 1973; Gaitzsch et al. 1995; Fig. 3). As a consequence, the definition of the Flechtingen Formation by Gaitzsch et al. (1995), based on Burchardt and Eisenächer (1970), Benek et al. (1973), Walter and Gaitzsch (1988), and Hoth et al. (1973), must be revised. The formation encompasses the siliciclastic and volcanoclastic Bodendorf and Eiche Members separated by the "lower andesitoids I and II" (Gaitzsch et al. 1995). As already shown by Awdankiewicz et al. (2004), these andesitoids do not depict subaerial flows, as assumed before, but intrusive sills. Consequently, the Bodendorf and Eiche members represent large sedimentary rafts, trapped inside the sills (Fig. 2). Thus, their primary position remains still unknown. Based on distinct lithological similarities, the volcanoclastics of the Mammendorf quarry depict a lateral equivalent of the Eiche Member. Hence, the outcrop indicates that the Eiche Member was overlying the Variscian folded early Carboniferous turbiditic greywackes of the Magdeburg Formation (Visean–Serphukovian) with an angular and structural unconformity. Following the above-mentioned authors, for the Bodendorf Member a lithostratigraphical position below the Eiche Member is assumed. However, a stratigraphic concordance of all three units (Mammendorf volcanoclastics, Eiche and Bodendorf Members) may not be excluded.

The Süplingen Formation was deposited directly on the exposed turbiditic series of early Carboniferous age (Visean–Serphukovian; Paech 1973; Paech et al. 1973), as well. Based on the modal composition and maturity, sediments of this formation differ completely from those of the Bodendorf and Eiche Members (Flechting Fm.). Grey facies and typical micritic shallow-lacustrine limestone beds (Gebhardt 1988) of the Süplingen Formation support the late Carboniferous (Stephanian–Gzhelian) age but tend to be somewhat older than the Flechtingen Formation. Single thin pyroclastic horizons in the Süplingen Formation may herald the beginning of the strong volcanism in the FVC, which initiated with pyroclastic fallout of the Eiche Member and cumulated in depositing thick sheets of welded ignimbrites of the Roxförde Formation at 302 ± 3 Ma. Simultaneously, this age indicates initiation of volcanic activity of the Flechtingen-Altmark Subprovince in the Southern Permian Basin. The onset of deposition of the Süplingen and Flechtingen Formations on the Variscian country-rock point to an already deeply eroded Variscian orogen/morphogen, but with a still differentiated and active topography.

Volcanogenetic model of the FVC

Awdankiewicz et al. (2004) presented the first comprehensive volcanogenetic model of the FVC, including the re-interpreted andesitic magma sheets, which have been emplaced as sills into the basal volcanoclastic series during the post-ignimbritic eruption phase. This model is confirmed and extended by this study. Including the stratigraphic implications gained from the sediments of the Süplingen and Flechtingen Formations, the volcanic activity can be differentiated into at least seven stages (Fig. 9).

Stage I is represented by single silicic pyroclastic horizons of the Süplingen Formation, heralding the initiation of the major volcanic activity. During stage II, volcanic activity was distinctly rising by producing major silicic fallout deposits during the Flechtingen Formation (Eiche Member) at 302 ± 3 Ma. Stage III indicates the cumulation of the eruption, which has produced the voluminous silicic and hot ignimbrites of the Roxförde Formation. The upper Holzmühlental ignimbrite reveals the same radiometric age as the fallout deposits of the Eiche Member (Breitkreuz and Kennedy 1999). Thus, we are able to conclude that (1) the chronostratigraphic age of 302 ± 3 Ma for the initial and major phase of the FVC volcanism is consolidated by two independent radiometric approaches, and (2) the fallout deposits of the Eiche Member are co-genetic with the ignimbritic deposits of the Roxförde Formation, whereas not much time has passed between both eruption stages. During the

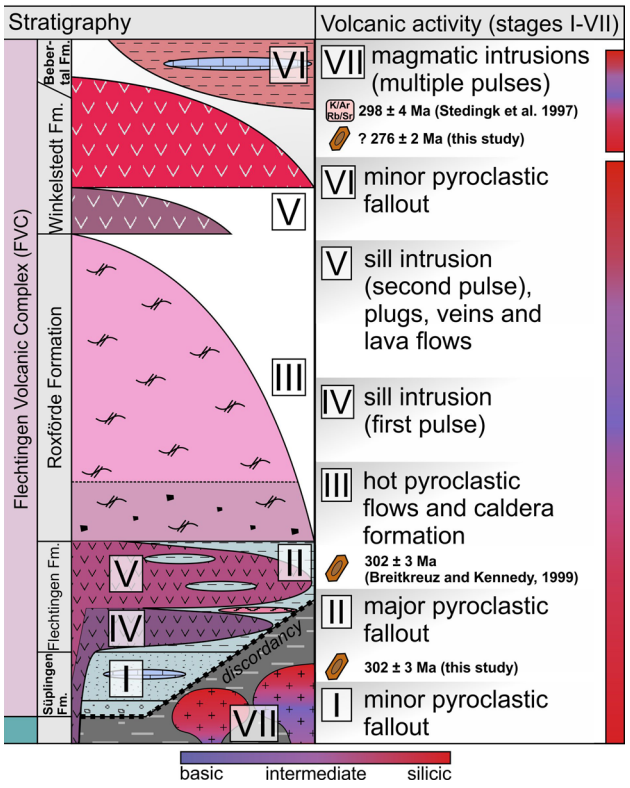

Fig. 9 Volcanogenetic model, corresponding eruption phases and magma compositional development of the FVC

major eruption, a large sag caldera formed accommodating the > 400 m of welded Flechtingen ignimbrites. Shortly after caldera formation, the pyroclastic sheet has been lifted up at least 200 m, caused by the emplacement of the andesitic sills.

In the following stage IV, intermediate to basic magma intruded the Flechtingen Formation, in a first pulse, forming the "lower andesitoid I" (Awdankiewicz et al. 2004), which migrated at least 25 km from the proposed conduit(s) in a south-eastern direction. However, the position of the conduit(s) feeding the Flechtingen Sill is poorly constrained. We can only speculate that the andesitic melts rose in an area spatially related to the Flechtingen caldera and to the Flechtingen Granite. The andesitic magma ascended through the consolidated early Carboniferous turbidites and formed a sill complex close to the base of the overlying semi- to unconsolidated volcaniclastic series, a stratigraphic level that resembled a major strength discontinuity of the host. These discontinuities have been observed to serve as preferred cites for sill initiation (Hogan et al. 1998).

During stage V, in a second magma pulse the "lower andesite II" was intruding at the same stratigraphic level as the "lower andesitoid I" (Awdankiewicz et al. 2004). Due to a high phenocryst content, its spatial distribution was lower compared to the "lower andesitoid I". Simultaneously, silicic to intermediate magma was extruded forming veins, plugs and locally restricted lava flows (Awdankiewicz et al. 2004), which are represented by the Winkelstedt Formation (Gaitzsch et al. 1995). During stage IV and V, a considerable magma volume was intruding the Flechtingen Formation, regarding the whole sill complex. Assuming an overall ellipsoid geometry for the Flechtingen sill complex we may define, based on our field data, two of its half axis as 0.1 km (half thickness) and 10 km (half-length). However, no constraints for the half-width are known. A global compilation on mafic sill geometry shows that sills with c. 200 m thickness have typically a volume in the order of 10 km^3 (Cruden et al. 2018). Taking this volume estimate into the ellipsoid calculation, a half-width of 1.2 km results. Thus, presumably the Flechtingen sill complex resembles a NW–SE-oriented ellipsoid with a length, width and thickness of 20 km, 2.4 km and 0.2 km, respectively. Benek et al. (1996) assumed a volume of 3750 km^3 for all andesitic rocks of the Subhercyn-Flechtingen-Altmark region, of which the Flechtingen Sill apparently is just one unit.

Stage VI is characterised by minor silicic fallout deposits in the Bebertal Formation, which indicates the cessation of volcanic activity of the FVC.

Emplacement of the Flechtingen and Roxförde granitic intrusions is evidenced to have been taken place after deposition of the volcanoclastics of the Süplingen Formation at 302 ± 3 Ma, as the sediments show contact metamorphic overprint. Here, we present two new U/Pb radiometric ages for the Flechtingen and Roxförde Granite (see supplement). The radiometric age of 293 ± 2 Ma for the Flechtingen Granite is distinctly younger than the assumed emplacement age of 298 ± 4 Ma from biotite dating (Stedingk et al., 1997). Thus, the age presented in this study seems to indicate zircon growth within the Flechtingen batholith after emplacement, which is likely regarding its dimensions. This is in accordance with younger K/Ar and Rb/Sr ages presented by Stedingk et al. (1997). The U/Pb radiometric age of 276 ± 2 Ma for the Roxförde Granite is distinctly younger compared to the ages of the Flechtingen Granite and might either reflect a distinctly later intrusion or a post-intrusion recrystallisation event caused by fluorine hydrothermals, which was discussed by Bauer et al. (1995). In conclusion, post-volcanic emplacement of the Flechtingen and Roxförde Granites is suggested to represent stage VII of the FVC activity, triggered by the injection of several basic-intermediate to silicic magma pulses, which is reflected by the heterogenous lithology of the Flechtingen Granite.

To date, origin and evolution of the FVC magma remain speculative and must be clarified by future mineralogical and geochemical approaches. Important questions to be addressed are the origin of the chemically heterogenous magma from crustal and/or mantle regions (Awdankiewicz

et al. 2004), the significance of magmatic garnet in the ignimbrites and granites, as well as the relation of granite formation to the volcanic eruption. Finally, the understanding of the FVC, representing another large volcanic complex in the late Paleozoic of Central Europe, will contribute to clarify the driving forces behind the magmatic flare-up during this time interval.

Conclusions

1. The andesite sheet in the Mammendorf quarry is clearly identified as subvolcanic intrusion forming a sill that intruded strata-concordant in between turbiditic sedimentary rocks of early Carboniferous age and late Pennsylvanian volcanoclastic deposits of the Flechtingen Formation—a level that represents a major strength discontinuity favourable for sill initiation.
2. The Mammendorf sill is part of the sill complex described by Awdankiewicz et al. (2004), which extends more than 25 km from the Bodendorf quarry to Mammendorf and was emplaced during the post-ignimbritic phase of the Flechtingen Volcanic Complex (FVC).
3. As a result of emplacement, two different types of magma–host rock interaction occurred: (a) brittle deformation at the basal contact with early Carboniferous sedimentary rocks, indicated by sharp magma–host rock contacts and magma injection in between host-rock layers; (b) large-scale brittle deformation of consolidated volcanoclastic sediment at the upper contact, but local fluidisation of less consolidated sediments at the direct contact, leading to magma-sediment mingling of juvenile andesitic clasts formed by hydromagmatic explosions (peperite), and vertical fluid migration through the sedimentary succession forming a variety of secondary mineralisation.
4. The volcanoclastic deposits of the Mammendorf quarry reveal a radiometric age of 302 ± 3 Ma, suggesting a cogenetic relation to the FVC ignimbrites of the Roxförde Fm. (Breitkreuz and Kennedy 1999). Simultaneously, the new radiometric age consolidates the late Pennsylvanian stratigraphic age of the initial and major phase of the FVC volcanism.
5. Based on lithological similarities, the Mammendorf volcanoclastics represent a genetic and stratigraphic equivalent of the Eiche Member, and are thus part of the Flechtingen Formation, defined by Gaitzsch et al. (1995). These deposits most likely once represented a more or less continuous sedimentary succession before they were spatially isolated by the intruding sill system.
6. Pyroclastic horizons of the Süplingen Formation may herald volcanic activity of the FVC and the whole Flechtingen-Altmark Subprovince in the Southern Permian Basin, which initiated at 302 ± 3 Ma in the Flechtingen Formation. It cumulated with deposition of the Roxförde Formation (302 ± 3 Ma) and ceased with emplacement of the Flechtingen and Roxförde Granites between 298 ± 4 Ma and probably 276 ± 2 Ma.

Electronic supplementary material The online version of this article (https://doi.org/10.1007/s00531-020-01911-y) contains supplementary material, which is available to authorized users.

Acknowledgements We thank Ute Gebhardt, Karlsruhe, for sharing expertise in stratigraphy of the Flechtingen–Roßlau Block, Michael Buchwitz and Frank Trostheide, both Magdeburg, for field discussions and logistic support. We would like to acknowledge Sascha Wienbrock, Cronenberger Steinindustrie (Franz Triches GmbH & co KG), for a great cooperation, giving access to the Mammendorf quarry and to exploration drill cores. Financial support was provided by the Landesamt für Geologie und Bergbau (LAGB), Sachsen–Anhalt. We would like to thank the technical staff from the Geological Institute (TU Bergakademie Freiberg) for thin sectioning and sample preparation for radiometric dating. We thank Lothar Viereck for his quality-improving review. Joerg W. Schneider and Birgit Gaitzsch thank the Kazan Federal University, Russia, for support in the frame of the state assignment no. 5.2192.2017/4.6.

Author contributions All authors contributed to the study conception and design. Material preparation, data collection and analysis were performed by LL, JB, JWS, K-PS, UL and MH. The first draft of the manuscript was written by LL and all authors commented on previous versions of the manuscript. JWS, BG, B-CE and CB added text passages in later versions of the manuscript. All authors read and approved the final manuscript.

Funding Open Access funding enabled and organized by Projekt DEAL. Financial support was provided by the Landesamt für Geologie und Bergbau (LAGB), Sachsen-Anhalt, and the TU Bergakademie Freiberg (Geological Institute).

Availability of data and material Primary data presented on radiometric dating are accessible in the IJES data repository.

Compliance with ethical standards

Conflict of interest The authors declare that they have no competing interests.

Ethical approval The manuscript is exclusively submitted to the IJES. The submitted work is original and is not split into several parts to increase the quantity of submissions to various journals. Data, text or theories by other authors are marked as their own literary property. All further ethic approvals named in the IJES guidelines are considered.

References

Arthaud F, Matte P (1977) Late Paleozoic strike-slip faulting in Southern Europe and Northern Africa; results of a right-lateral shear zone between the Appalachians and the Urals. Geol Soc Am Bull 88:1305–1320

Awdankiewicz M, Breitkreuz C, Ehling BC (2004) Emplacement textures in Late Paleozoic andesite sills of the Flechtingen–Roßlau Block, north of Magdeburg (Germany). In: Breitkreuz C, Petford N (eds) Physical geology of high-level magmatic systems, vol 234. Geol Soc London Spec Pub, pp 51–66

Bachmann GH, Ehling BC, Eichner R, Schwab M (2008) Geologie von Sachsen–Anhalt. E. Schweitzerbart'sche Verlagsbuchhandlung, Stuttgart

Barthel M, Katzung G, Sigeneger W, Uerckwitz G (1982) Pflanzenfunde aus dem Autun bei Bebertal (Flechtingen–Roßlauer Scholle). Z Geol Wiss 10:1381–1385

Bauer M, Schust F, Matheis G (1995) The hidden granitic intrusions of Flechtingen and Roxförde (NE-Rhenohercynian Zone). Zbl Geol Paläont T I(5/6):553–560

Benek R (1995) Late Variscan calderas/volcanotectonic depressions in eastern Germany. Terra Nostra 7:16–19

Benek R, Paech HJ, Schirmer B (1973) Zur Gliederung der permosilesischen Vulkanite der Flechtinger Scholle. Z Geol Wiss 1:867–878

Benek R, Kramer W, McCann T, Scheck M, Negendank JFW, Korich D, Huebscher HD, Bayer U (1996) Permo-Carboniferous magmatism of the Northeast German Basin. Tectonophys 266:379–404

Breitkreuz C, Kennedy A (1999) Magmatic flare-up at the Carboniferous/Permian boundary in the NE German Basin revealed by SHRIMP zircon ages. Tectonophys 302:307–326

Breitkreuz C, Mock A (2004) Are laccolith complexes characteristic of transtensional basin systems?—Examples from Permocarboniferous Central Europe. In: Breitkreuz C, Petford N (eds) Physical geology of high-level magmatic systems, vol 234. Geol Soc London Spec Pub, pp 13–32

Breitkreuz C, Kennedy A, Geissler M, Ehling BC, Kopp J, Muszynski A, Protas A, Stouge S (2007) Far Eastern Avalonia: its chronostratigraphic structure revealed by SHRIMP zircon ages from Upper Carboniferous to Lower Permian volcanic rocks (drill cores from Germany, Poland and Denmark). Geol Soc Am Spec Pap 423:173–190

Breitkreuz C, Ehling BC, Pastrik N (2018) The subvolcanic units of the Late Paleozoic Halle Volcanic Complex, Germany: geometry, internal textures and emplacement mode. In: Breitkreuz C, Rocchi S (eds) Physical geology of shallow magmatic systems—Dykes, sills and laccoliths. Adv Volcanol, Springer, New York, pp 295–308

Brink HJ (2005) Liegt ein wesentlicher Ursprung vieler großer Sedimentbecken in der thermischen Metamorphose ihrer Unterkruste? Das norddeutsche Permbecken in einer globalen Betrachtung. Z deut Geow 156:275–290

Brink J (2013) Geometrie und Faziesanalyse des spätpaläozoischen Andesitoid-Körpers im Bereich des Steinbruchs Mammendorf nordwestlich von Magdeburg. BSc thesis, TU Bergakademie Freiberg

Brown DJ, Bell BR (2007) How do you grade a peperite? J Volcanol Geotherm Res 159:409–420

Buchwitz M, Luthardt L, Marchetti L, Trostheide F, Voigt S, Schneider JW (2017) A Middle to Late Permian tetrapod tracksite from northern Germany. In: Bordy E (ed) 2nd Conference of continental ichnology, Nuy Valley, Western Cape, South Africa, 1st–4th October 2017. Abstract Book 15

Burchardt I, Eisenächer L (1970) Neue Ergebnisse zur Gliederung der Vulkanitserie im Gebiet des Flechtinger Höhenzuges (Subherzyne Scholle). Geologie 19:813–825

Busby-Spera CJ, White JDL (1987) Variation in peperite textures associated with differing host-sediment properties. Bull Volcanol 49:765–775

Casas-García R, Rapprich V, Breitkreuz C, Svojtka M, Lapp M, Stanek KP, Hofmann M, Linnemann U (2019) Lithofacies architecture, composition, and age of the Carboniferous Teplice Rhyolite (German-Czech border): insights into the evolution of the Altenberg-Teplice Caldera. J Volc Geotherm Res 386:106662

Cruden AR, McCaffrey KJW, Bunger AP (2018) Geometric scaling of tabular igneous intrusions: implications for emplacement and growth. In: Breitkreuz C, Rocchi S (eds) Physical geology of shallow magmatic systems—Dykes, sills and laccoliths. Springer, New York, pp 11–38

Förster HJ, Romer RL (2010) Carboniferous magmatism. In: Linnemann U, Romer RL (eds) Pre-Mesozoic Geology of Saxo-Thuringia—from the Cadomian Active Margin to the Variscan Orogen. Schweizerbart, Stuttgart, pp 287–308

Frei D, Gerdes A (2009) Precise and accurate in situ U–Pb dating of zircon with high sample throughput by automated LA-SF-ICP-MS. Chem Geol 261(3):261–270

Gaitzsch B, Ellenberg J, Lützner H, Benek R (1995) Stratigraphie des Rotliegend in Oberflächenaufschlüssen—Flechtinger Scholle. In: Plein E (ed): Stratigraphie von Deutschland I—Norddeutsches Rotliegendbecken, Rotliegend-Monographie Teil II, vol 183. Courier Forschungsinstitut Senckenberg, pp 84–96

Gebhardt U (1988) Mikrofazies und Paläontologie biogener Karbonate der unteren Mansfelder Schichten (Oberkarbon, Stefan). Hall Jb Geowiss 13:5–21

Gebhardt U, Schneider JW, Hoffmann N (1991) Modelle zur Stratigraphie und Beckenentwicklung im Rotliegend der Norddeutschen Senke. Geol Jb A 127:405–427

Geißler M, Breitkreuz C, Kiersnowski H (2008) Late Paleozoic volcanism in the central part of the Southern Permian Basin (NE Germany, W Poland): facies distribution and volcano-topographic hiati. Int J Earth Sci 97:973–989

Gerdes A, Zeh A (2006) Combined U–Pb and Hf isotopes LA-MC-ICP-MS analysis of detrital zircons—comparison with SHRIMP and new constraints for the provenance and age of an Armorican metasediment in Central Germany. Earth Planet Sci Lett 249:47–61

German stratigraphic commission, Menning M, Hendrich A (eds) (2016) Stratigraphic Chart of Germany 2016. Geoforschungszentrum, Potsdam

Gersemann J (1989) Bau und Entwicklung des permokarbonen Stockwerkes in Ostniedersachsen. Bswg Geol-paläont Diss 9:1–114

Gihm YS, Kwon CW (2017) Textural variations and fragmentation processes in peperite formed between felsic lava flow and wet substrate: An example from the Cretaceous Buan Volcanics, southwest Korea. J Volcanol Geotherm Res 331:92–101

Gilbert JS, Rogers NW (1989) The significance of garnet in the Permo-Carboniferous volcanic rocks of the Pyrenees. J Geol Soc 146:477–490

Harangi SZ, Downes H, Kósa L, Szabó CS, Thirlwall MF, Mason PRD, Mattey D (2001) Almandine garnet in calc-alkaline volcanic rocks of the Northern Pannonian Basin (Eastern–Central Europe): geochemistry, petrogenesis and geodynamic implications. J Petrol 42(10):1813–1843

Haug ØT, Galland O, Souloumiac P, Souche A, Guldstrand F, Schmiedel T (2017) Inelastic damage as a mechanical precursor for the emplacement of saucer-shaped intrusions. Geology 45:1099–1102

Hoffmann U, Breitkreuz C, Breiter K, Sergeev S, Stanek KP, Tichomirowa M (2013) Carboniferous-Permian volcanic evolution in Central Europe—U/Pb ages of volcanic rocks in Saxony (Germany) and northern Bohemia (Czech Republic). Int J Earth Sci 102:73–99

Hogan JP, Price JD, Gilbert MC (1998) Magma traps and driving pressure: consequences for pluton shape and emplacement in an extensional regime. J Struct Geol 20(9/10):1155–1168

Hoth K, Paech HJ, Kampe A (1973) Hinweise auf Intrusivkörper im nördlichen Teil der Flechtingen–Roßlauer Scholle. Z Geol Wiss 1:861–866

Hutton DHW (2009) Insights into magmatism in volcanic margins: bridge structures and a new mechanism of basic sill emplacement—Theron Mountains, Antarctica. Petrol Geosci 15:269–278

Jackson SE, Pearson NJ, Griffin WL, Belousova EA (2004) The application of laser ablation-inductively coupled plasma-mass spectrometry to in situ U–Pb zircon geochronology. Chem Geol 211(1):47–69

Jamtveit B, Svensen H, Podladchikov Y, Planke S (2004) Hydrothermal vent complexes associated with sill intrusions in sedimentary basins. Phys Geol High Level Magmat Syst 234:233–241

Kahlert E (1973) Die biostratigraphische Einstufung der "Süplinger Schichten" (Flechtinger Höhenzug). Z Geol Wiss 1:851–859

Kelch H-J, Paulus B (1980) Die Tiefbohrung Velpke-Asse Devon 1. Geol Jahrb A 57:3–175

Kennedy BM, Holohan EP, Stix J, Gravley GM, Davidson JRJ, Colea JW (2018) Magma plumbing beneath collapse caldera volcanic systems. Earth Sci Rev 17:404–424

Kokelaar BP (1982) Fluidization of wet sediments during the emplacement and cooling of various igneous bodies. J Geol Soc Lond 139:21–33

Korich D (1992) Zur Vulkanologie und Korrelation der permosilesischen Vulkanite im Darß-Uckermark-Eruptivkomplex/Nordostdeutschland. Z Geol Wiss 20:467–473

Kroner U, Romer RL (2013) Two plates—many subduction zones: the Variscan orogeny reconsidered. Gondwana Res 24:298–329

Kroner U, Roscher M, Romer RL (2016) Ancient plate kinematics derived from the deformation pattern of continental crust: Paleo- and Neo-Tethys opening coeval with prolonged Gondwana-Laurussia convergence. Tectonophys 681:220–233

Legler B (2006) Faziesentwicklung im Südlichen Permbecken in Abhängigkeit von Tektonik, eustatischen Meeresspiegelschwankungen des Proto-Atlantik und Klimavariabilität (Oberrotliegend, Nordwesteuropa). SDGG 47

Legler B, Schneider JW, Gebhardt U, Merten D, Gaupp R (2011) Lake deposits of moderate salinity as sensitive indicators of lake level fluctuations: Example from the Upper Rotliegend saline lake (Middle–Late Permian, Northeast Germany). Sediment Geol 234:56–69

Litt T, Wansa S (2008) Quartär. In: Bachmann et al (eds) Geologie von Sachsen-Anhalt. Schweitzerbart'sche Verlagsbuchhandlung, Stuttgart, pp 293–325

Lorenz V, Haneke J (2004) Relationship between diatrems, dykes, sills, laccoliths, intrusive-extrusive domes, lava flows, and tephra deposits with unconsolidated water-saturated sediments in the late-Variscan Saar-Nahe-Basin, SW Germany. In: Breitkreuz C, Petford N (eds) Physical geology of high-level magmatic systems, vol 234. Geol Soc London Spec Pub, pp 75–124

Ludwig KR (2001) User Manual for isoplot/Ex. rev. 2.49. Berkeley Geochronol Center Spec Publ 1a, pp 1–56

Luthardt L (2013) Kartierung der Pyroklastit-Sediment-Folge im Steinbruch Mammendorf, Flechtingen Block. Msc mapping report. TU Bergakademie Freiberg

Marx J, Huebscher HD, Hoth K, Korich D, Kramer W (1995) Vulkanostratigraphie und Geochemie der Eruptivkomplexe. In: Plein E (ed) Stratigraphie von Deutschland I—Norddeutsches Rotliegendbecken, Rotliegend-Monographie Teil II, vol 183. Courier Forschungsinstitut Senckenberg, pp 54–83

Meinhold G, Morton AC, Fanning CM, Frei D, Howard JP, Phillips RJ, Strogen D, Whitham AG (2011) Evidence from detrital zircons for recycling of Mesoproterozoic and Neoproterozoic crust recorded in Paleozoic and Mesozoic sandstones of southern Libya. Earth Planet Sci Lett 312(1):164–175

Müller A (2011) Der Steinbruch Mammendorf NW Magdeburg—Ein Felslitoral der unteroligozänen Nordsee. Geol Saxonica 57:3–120

Obst K, Katzung G (2000) Die magmatischen Gänge am Südrand des Kristallins von Ruhla-Brotterode (Thüringer Wald)—Herkunft der Magmen, Aufstieg und Platznahme im variszischen Spannungsfeld. Z dt Geol Ges 151:441–470

Paech HJ (1973) Zur Sedimentologie der Grauwacken-Pelit-Wechsellagerung der Flechtinger Scholle (Bezirk Magdeburg). Z Geol Wiss 1:805–813

Paech HJ, Eisenächer L, Burchhardt I (1973) Neue Ergebnisse zur Geologie der Süplinger Schichten (Flechtinger Scholle). Z Geol Wiss 1:831–847

Paulick H, Breitkreuz C (2005) The Late Paleozoic felsic lava-dominated large igneous province in North East Germany: volcanic facies analysis based on drill cores. Int J Earth Sci 94:834–850

Repstock A, Heuer F, Im J, Hübner M, Schulz B, Breitkreuz C, Gilbricht S, Fischer F, Lapp M (2018) A Late Paleozoic Snake River-type ignimbrite (Planitz vitrophyre) in the Chemnitz Basin, Germany: textural and compositional evidence for complex magma evolution in an intraplate setting. J Volcanol Geotherm Res 369:35–49

Repstock A, Heuer F, Im J, Hübner M, Schulz B, Breitkreuz C, Gilbricht S, Fischer F, Lapp M (2019) A Late Paleozoic Snake River-type ignimbrite (Planitz vitrophyre) in the Chemnitz Basin, Germany: textural and compositional evidence for complex magma evolution in an intraplate setting. J Volc Geotherm Res 369:35–49

Schofield NJ, Brown DJ, Magee C, Stevenson CT (2012) Sill morphology and comparison of brittle and non-brittle emplacement mechanisms. J Geol Soc Lond 169:127–141

Schmiedel T, Breitkreuz C, Görz I, Ehling BC (2015) Geometry of laccolith margins: 2D and 3D models of the Late Paleozoic Halle Volcanic Complex (Germany). Int J Earth Sci 104:323–333

Schneider JW, Lucas SG, Scholze F, Voigt S, Marchetti L, Klein H, Opluštil S, Werneburg R, Golubev VK, Barrick JE, Nemyrovska T, Ronchi A, Day MO, Silantiev VV, Rößler R, Saber H, Linnemann U, Zharinova V, Shen SZ (2019) Late Paleozoic-early Mesozoic continental biostratigraphy—links to the Standard Global Chronostratigraphic Scale. Paleoworld 531:53

Schreiber A (1960) Das Rotliegende des Flechtinger Höhenzuges. Freib Forschungsh C82:1–132

Seckendorff V von (2012) Der Magmatismus in und zwischen den spätvariscischen permokarbonen Sedimentbecken in Deutschland. In: Deutsche Stratigraphische Kommission (eds) Stratigraphie von Deutschland X. Rotliegend. Teil I: Innervariscische Becken, vol 61. Schriftenr Deut Ges Geow, pp 743–860

Sircombe KN (2004) Age Display: an Excell workbook to evaluate and display univariate geochronological data using binned frequency histograms and probability density distributions. Comput Geosci 30:21–31

Skilling IP, White JDL, McPhie J (2002) Peperite: a review of magma-sediment mingling. J Volcanol Geotherm Res 114:1–17

Sláma J, Košler J, Condon DJ, Crowley JL, Gerdes A, Hanchar JM, Horstwood MSA, Morris GA, Nasdala L, Norberg N, Schaltegger U, Schoene B, Tubrett MN, Whitehouse MJ (2008) Plešovice zircon—a new natural reference material for U–Pb and Hf isotopic microanalysis. Chem Geol 249(1):1–35

Söllig A, Röllig G (1989) Geologische Karte der Deutschen Demokratischen Republik, Tektonische Karte 1:500,000, Zentrales Geologisches Institut (ZGI), Berlin

Stacey JS, Kramers JD (1975) Approximation of terrestrial lead isotope evolution by a two-stage model. Earth Planet Sci Lett 26:207–221

Stedingk K, Hess J, Bauer M (1997) Zur regionalen Position, Ausbildung und Alterstellung des Granits von Flechtingen. Z Geol Wiss 25:317–329

Svensen HH, Planke S, Neumann ER, Aarnes I, Marsh JS, Polteau S, Harstad CH, Chevallier L (2018) Sub-volcanic intrusions and the link to global climatic and environmental changes. In: Breitkreuz C, Rocchi S (eds) Physical Geology of Shallow Magmatic Systems. Adv Volcanol, pp 249–272

Timmerman MJ (2008) Palaeozoic magmatism. In: McCann T (ed) The geology of central Europe, vol 1: Precambrian and Palaeozoic. Geol Soc Lond, pp 665–748

Walter H, Gaitzsch B (1988) Beiträge zur Ichnologie limnisch-terrestrischer Sedimentationsräume, Teil II: *Diplichnites minimus* n. *ichnosp*. aus dem Permosiles des Flechtinger Höhenzuges. Freib Forschungsh C 427:73–84

Weyer D (1975) Biostratigrafie des Magdeburg-Flechtinger Kulms. Z Geol Wiss 3:547–589

White JDL, McPhie J, Skilling IP (2000) Peperite: a useful genetic term. Bull Volcanol 62:65–66